

2015

Phenotypic characterization of PNPase knockdown in *C. elegans*

Laura A. Lambert

Virginia Commonwealth University, laycockla@vcu.edu

Follow this and additional works at: <http://scholarscompass.vcu.edu/etd>



Part of the [Genetics Commons](#)

© The Author

Downloaded from

<http://scholarscompass.vcu.edu/etd/3757>

This Thesis is brought to you for free and open access by the Graduate School at VCU Scholars Compass. It has been accepted for inclusion in Theses and Dissertations by an authorized administrator of VCU Scholars Compass. For more information, please contact libcompass@vcu.edu.

PHENOTYPIC CHARACTERIZATION OF PNPASE KNOCKDOWN IN C. ELEGANS

A thesis submitted in partial fulfillment of the requirements for the degree of Master of Science
at Virginia Commonwealth University

by LAURA LAMBERT

Bachelor of Science, UVA 2008

Master of Arts in Teaching, JMU 2010

Director: RITA SHIANG, Ph.D.

ASSOCIATE PROFESSOR

DEPARTMENT OF HUMAN AND MOLECULAR GENETICS

Virginia Commonwealth University

Richmond, Virginia

April, 2015

Acknowledgement

I would like to thank first and foremost Dr. Rita Shiang, whose guidance, patience, and teaching has been instrumental in shaping my growth as a scientist. She has been an amazing mentor, teaching where needed and giving a verbal kick in the pants when deserved. I appreciate her willingness to talk not only about science, but also about life.

I would also like to thank my other committee members, Dr. Paul Fisher and Dr. Andrew Davies, for their guidance in seeing this project to fruition. Particular thanks go to Dr. Davies for his expertise in the *C. elegans* model system and the assistance he was able to provide.

Thank you also to Dr. Jill Bettinger and Dr. Laura Mathies, additional experts in the *C. elegans* model system. Dr. Bettinger was a valuable sounding board for many ideas and methods, and very helpful in troubleshooting difficult procedures. Dr. Mathies not only provided another set of ears to talk about this project, but also a steady set of hands that did our injections.

I cannot forget to thank the members, past and present, of the Shiang lab, without which lab would have been a much duller experience.

Lastly, a great deal of appreciation goes to my husband, Jordan, for his support throughout this process, and his patience with my odd hours, many absences, and frustration at experiments. Thank you also to my daughter, Sophia, who may not understand now, but who has been a great source of inspiration and motivation.

Table of Contents

	Page
Acknowledgements.....	ii
List of Tables and Figures.....	vi
List of Abbreviations.....	ix
Abstract.....	xi
 CHAPTER	
1. INTRODUCTION.....	1
a. PNPase.....	1
b. PNPase Structure.....	2
c. PNPase Localization.....	3
d. Functional Studies of hPNPaseold-35.....	3
i. Knockdown Studies	3
ii. Overexpression Studies	4
e. PNPase in Mitochondria	5
f. Human Diseases	6
g. Mitochondria	8
h. <i>C. elegans</i>	9

i. PNPase in <i>C. elegans</i>	11
j. Longevity Pathways	11
k. ROS.....	14
2. MATERIALS AND METHODS	15
a. <i>C. elegans</i> culture and maintenance.....	15
b. Bleaching of adult <i>C. elegans</i>	15
c. Generation of RNAi clone	15
d. RNAi	15
e. Extracting DNA from <i>C. elegans</i>	16
f. Extracting RNA from <i>C. elegans</i>	17
g. Generating cDNA from <i>C. elegans</i>	17
h. PCR	18
i. qPCR	19
j. Egg laying assays	19
k. Lifespan assays	20
l. Adult-initiation lifespan assays	21
m. PQ and NAC lifespan assays	21
n. ROS assay	22
o. Visualization of mitochondrial network	22
p. Imaging of mitochondria.....	23
q. NAD ⁺ /NADH assay	24
r. Creation of PNPase mutants	24
3. RESULTS	25

a.	Generation of a PNPase knockdown clone in <i>C. elegans</i>	25
b.	Characterization of Fertility and Fecundity of PNPase knockdown in <i>C. elegans</i>	26
c.	Characterization of Lifespan of PNPase knockdown in <i>C. elegans</i>	27
d.	PNPase knockdown acts to extend lifespan in a similar manner as Complex I and Complex III mutants.....	30
e.	PNPase knockdown extends lifespan by increasing ROS	33
f.	PNPase knockdown affects respiration	38
g.	PNPase knockdown increases mitochondrial network.....	39
h.	PNPase knockdown does not affect cristae structure.....	40
i.	PNPase knockdown increases the amount of polycistronic mitochondrial transcripts	42
j.	PNPase knockdown increases <i>fzo-1</i>	44
k.	Generation of PNPase mutant strains	45
4.	DISCUSSION	48
a.	PNPase knockdown in <i>C. elegans</i> increases lifespan	48
b.	PNPase knockdown increases ROS production	49
c.	PNPase knockdown increases the NAD ⁺ /NADH ratio	51
d.	PNPase knockdown affects mitochondrial network, morphology, and distribution	52
e.	PNPase knockdown increases mitochondrial polycistronic transcript accumulation	54
f.	Conclusions	55
	Literature Cited	58

List of Tables and Figures

	Page
Figure 1: Structure of PNPase	3
Figure 2: Summary of PNPase roles and subcellular localization.....	6
Figure 3: Relation of fusion and fission	9
Figure 4: Lifecycle of <i>C. elegans</i>	10
Figure 5: <i>C. elegans</i> longevity pathways	12
Table 1: Primer sequences and uses	18
Table 2: Primer pairs and annealing temperatures.....	18
Figure 6: Validation of PNPase knockdown	26
Figure 7: PNPase knockdown does not affect egg laying	27
Figure 8: PNPase knockdown extends lifespan in <i>C. elegans</i>	28
Table 3: Mean lifespans and p-values for trials A-C as seen in Figure 8	28
Figure 9: Adult initiation of RNAi produces inconsistent results	29
Table 4: Mean lifespans and p-values for trials A-D in Figure 9	30
Figure 10: Combining PNPase knockdown with three mitochondrial mutants reveals selectivity in lifespan extension pathway	31

Table 5: Mean lifespans and p-values for <i>isp-1</i> mutant animals on RNAi or control bacteria, corresponding to Figure 10A	32
Table 6: Mean lifespans and p-values for <i>clk-1</i> mutant animals on RNAi or control bacteria, corresponding to Figure 10B	33
Table 7: Mean lifespans and p-values for <i>nuo-6</i> mutant animals on RNAi or control bacteria, corresponding to Figure 10C	33
Figure 11: PQ does not further extend lifespan in knockdown animals	35
Table 8: Mean lifespans and p-values of worms exposed to paraquat corresponding to Figure 11, A-D	36
Figure 12: NAC abolishes lifespan extension seen in knockdown animals.....	37
Table 9: Mean lifespans and p-values of worms exposed to NAC corresponding to Figure 12, A-D	37
Figure 13: PNPase knockdown increases ROS production.	38
Figure 14: PNPase knockdown increases the NAD ⁺ /NADH ratio	39
Figure 15: PNPase knockdown increases the mitochondrial network	40
Figure 16: PNPase knockdown affects mitochondrial size but not cristae structure	41
Figure 17: Locations of genes and tRNAs in the <i>C. elegans</i> mitochondrial genome	43
Figure 18: PNPase knockdown increases polycistronic transcripts	44
Figure 19: PNPase knockdown increases <i>fzo-1</i> expression.....	45

Figure 20: PNPase deletion strains	46
Figure 21: Proposed mechanism for the downstream action of knockdown of <i>pnpt-1</i> in <i>C. elegans</i>	57

List of Abbreviations

ABS - absorption

Apaf-1 – apoptotic protease activating factor 1

ATP – adenosine triphosphate

clk-1 – clock abnormal protein 1

CRISPR – clustered regularly interspaced short palindromic repeats

DEPC – diethylpyrocarbonate

DIC – differential interference contrast

DNA – deoxyribonucleic acid

Drp1 – dynamin-related protein 1

ETC – electron transport chain

IFN – interferon

IGF-1 – insulin growth factor 1

IPTG – isopropyl β -D-1-thiogalactopyranoside

isp-1 – iron sulfur protein 1

Mfn1 – mitochondrial fusion protein 1

Mfn2 – mitochondrial fusion protein 2

M-MLV – moloney murine leukemia virus

MMP1 – metal metalloproteinase 1

MTS – mitochondrial targeting sequence

NAC – n-acetyl cysteine

NAD(H) – nicotinamide adenine dinucleotide

NGM – normal growth medium

Opa1 – optic atrophy 1

OXPHOS – oxidative phosphorylation

PCR – polymerase chain reaction

PNPase - Polyribonucleotide phosphorylase

PQ – paraquat

RBD – RNA binding domain

RNA – ribonucleic acid

ROS - Reactive Oxygen Species

RPH – Rnase PH

RT – reverse transcriptase

SOD2 – superoxide dismutase 2

TEM – transmission electron microscope

WLB – worm lysis buffer

ABSTRACT

PHENOTYPIC CHARACTERIZATION OF PNPASE IN *C. ELEGANS*

By Laura Lambert, B.S., M.A.T.

A thesis submitted in partial fulfillment of the requirements for the degree of Master of Science
at Virginia Commonwealth University

Virginia Commonwealth University, 2014

Major Director: Rita Shiang
Associate Professor, Department of Human and Molecular Genetics

The multifunctional exoribonuclease protein PNPase is implicated as a potential target for cancer therapy as well as causing mitochondrial disorders in humans, but there has yet to be a whole animal knockdown model created. In this study, *C. elegans* was used to investigate the effect of knocking down *pnpt-1*, the gene that encodes PNPase. It was discovered that *pnpt-1* knockdown significantly extends lifespan via an increase in superoxide production similar to other known mitochondrial lifespan extension pathways. Additionally, mitochondrial networks, size and respiration are affected indication of other mitochondrial dysfunction..

PNPase is also known to transport small RNAs into the mitochondria which in turn can affect mitochondria RNA splicing and translation of proteins involved in respiration. Further investigation showed a significant accumulation of polycistronic mitochondrial transcripts in knockdown animals. Lastly, this model has shown that PNPase knockdown is functionally comparable across species and is a viable model for future studies.

CHAPTER 1: INTRODUCTION

I. PNPase

PNPase, encoded by the gene PNPT1, is a highly conserved, nuclear-encoded 3'-5' exoribonuclease that localizes to the inner membrane space of the mitochondria as well as showing locations in the cytosol (Piwowarski et al, 2003; Chen et al, 2006; Leszczyniecka et al, 2002; Sarkar and Fisher, 2006). PNPT1 maps to 2p15-2p16.1 in humans, spanning 60 kb and containing 28 exons (Leszczyniecka et. al., 2003). *hPNPase^{old-35}* (human *PNPase*) was first discovered as an upregulated gene in an overlapping pathway screen intended to identify genes that were co-regulated in senescent progeroid fibroblasts and terminally differentiated HO-1 human melanoma cells (Leszczyniecka et al., 2002). In this screen, there were 75 genes identified and designated *old-1* through *old-75*. *old-35* was identified as showing significant homology to PNPase from other species, and thus labeled as human PNPase, or *hPNPase^{old-35}* (Leszczyniecka et. al., 2002). This multi-functional enzyme has been shown to have a role in specifically degrading c-myc mRNA (Sarkar et al., 2003; Sarkar et. al., 2005), miR-221, miR-222, and miR-106b (Das et. al., 2010), and regulating translocation of small RNAs into the mitochondria, such as MRP (mitochondrial RNA processing), 5S rRNA, and RNase P (Wang et al., 2010; Wang et al., 2012). At the transcriptional level, it has been found to be induced by type I interferons (IFN- α and β). An IFN-stimulated response element (ISRE) was identified in

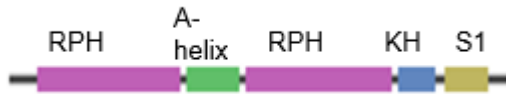
the promoter of hPNPase^{old-35}, and mutating this site eliminated induction of gene expression (Leszczyniecka et al., 2003).

II. PNPase Structure

PNPase is an evolutionarily conserved protein and is found in the majority of organisms from bacteria and plants to humans with the exception of fungi, trypanosomes and the entire domain Archaea (Sarkar and Fisher, 2006). PNPase in bacteria, humans, and plants have five conserved motifs: two RNase PH (RPH) domains at the amino terminal separated by an α -helix unique to PNPase and two C-terminal RNA binding domains (RBD) (KH and S1) (Figure 1A) (Symmons et al 2000; Leszczyniecka et al 2002; Raijmakers et al 2002; Symmons et al 2002; Leszczyniecka et al 2004). PNPase in *C. elegans* has the two RPH domains and the two C-terminal RBD but lacks the α -helix (Figure 1B). Plants contain an N-terminal chloroplast-transit peptide (cTP) or a mitochondrial-targeting sequence (MTS), while other organisms contain only the N-terminal MTS. Deletion studies in bacteria have shown that deletion of either the RBD, KH or S1 domains will reduce the specific activity of PNPase by 19-fold (KH) or 50-fold (S1). Deletion of both domains reduces activity to 1% (Stickney et al., 2005).

In humans, the PNPase protein is 783 amino acids long, with a weight of approximately 86 kDa. In its primary location, the mitochondria, it assembles into a homotrimer or a dimer of two homotrimers (Piwowarski et. al., 2003; Rainey et. al., 2006). When attempting to determine the minimum active region, mutation analysis showed that both RPH domains have equal enzymatic activity, and the presence of either one is sufficient for complete enzymatic activity. Additionally, hPNPase maintains enzymatic activity even when both RBDs have been deleted, indicating that the RPH domains may play a role in RNA binding in humans (Sarkar et. al., 2005).

A:



B:



Figure 1: Structure of PNPase A) In humans, there are 2 RNase PH (RPH) domains separated by an alpha-helix specific to PNPase followed by two RNA binding domains: KH and S1. B. Structure of PNPase in *C. elegans*: the two RPH domains are present as are the two RNA binding domains. The intervening alpha helix absent. (www.ncbi.nlm.nih.gov)

III. PNPase Localization

The MTS at the amino terminus of human PNPase localizes it to the mitochondria (Piwowarski et. al., 2003). Subfractionation studies further localized PNPase to the mitochondrial inner membrane space, specifically as an inner membrane bound peripheral protein (Chen et. al., 2006). PNPase is imported to the inner membrane space via an i-AAA protease Yme-1 dependent mechanism (Rainey et. al., 2006). Further studies have shown that hPNPase^{old-35} also localizes to the cytoplasm where it can degrade specific mRNA and miRNAs (Leszczyniecka et. al., 2002; Sarker et. al., 2003; Chen et. al., 2006; Das et. al., 2010).

IV. Functional Studies of hPNPase^{old-35}

a. Knockdown Studies

In vivo studies have indicated that total knockout of Pnpt1 in mice is embryonic lethal, showing its importance in development. A targeted liver knockout results in a decrease in the activity of the respiratory chain as well as causing disordered, circular, and smooth mitochondrial cristae (Wang et al., 2010). Additionally, PNPase knockdown in a melanoma cell line HEK-293T results in filamentous and granular mitochondria, a decrease in membrane

potential, and a decrease in the enzymatic activity of the respiratory complexes (Chen et al., 2006).

b. Overexpression Studies

Overexpression studies with *hPNPase*^{old-35} in HO-1 cells was performed in two different ways in order to investigate the mechanism of growth inhibition: slow and sustained overexpression via a low multiplicity of an adenoviral vector and rapid overexpression via a high multiplicity of an adenoviral vector. The results showed that there were different phenotypes for each method of overexpression. Slow and sustained overexpression, initiated to determine the mechanism behind inhibition of colony formation seen in HO-1 cells, resulted in growth inhibition and induction of a senescent-like phenotype, which ultimately resulted in apoptosis. Analysis of the cell cycle of these cells indicated that there was an initial G1/S or G2/M arrest followed by apoptosis (Sarkar et. al., 2003; Sarkar et. al., 2005; Van Maerken et al., 2009). Conversely, rapid overexpression, investigated to further investigate the mechanism behind PNPase overexpression induced growth arrest, promoted apoptosis without any accompanying cell-cycle changes (Sarkar et al., 2003).

Further, slow and sustained overexpression downregulated *c-myc* mRNA and protein, a key mediator in the G1/S transition. It was shown that *c-myc* overexpression will protect against cell death caused by overexpression of *hPNPase*^{old-35} (Sarkar et. al., 2003). It is thought that *hPNPase*^{old-35} specifically recognizes *c-myc* mRNA via the 3' UTR, as *c-myc* mRNA with no 3'UTR was resistant to degradation by *hPNPase*^{old-35} (Sarkar et. al., 2003; Sarkar et. al., 2006). As no RNA-binding site has been identified in PNPase from any species, it is thought that secondary structure in RNA may be the determining factor in determining specificity (Sohki et. al., 2013). Not only is *c-myc* specifically degraded, but it has been found that *hPNPase*^{old-35}

overexpression specifically degrades certain mature miRNA species such as miR-221, miR-222, and miR-106b (Das et. al., 2010). miR-221 is frequently overexpressed in a variety of human cancers, targeting a large set of 602 genes involved in oncogenic pathways (Lupini et. al., 2013). miR-222 is additionally found to be upregulated in a variety of cancers and has been found to target MMP1 (metal matrix protease 1) and SOD2 (superoxide dismutase 2) (Liu et. al., 2009). Lastly, miR-106b has been found to target a number of tumor suppressor genes (Liu et. al., 2014). Given the role these miRNAs play in cancer progression, elevated hPNPase^{old-35} may prove to be an attractive anti-cancer target.

V. PNPase in Mitochondria

Given the localization of hPNPase^{old-35} in the mitochondria, there have been multiple studies initiated to determine if hPNPase^{old-35} plays a role in mitochondrial homeostasis. Overexpression studies have indicated that the mitochondrial location of hPNPase^{old-35} plays a role in reactive oxygen species (ROS) induction (Sarkar et. al., 2004; Sarkar and Fisher, 2006). A change in the mitochondria is observable in knockdown and knockout experiments. Knockdown in HEK293T cells causes mitochondria to become filamentous and granular shaped, as well as decreasing membrane potential and reducing enzymatic activities of coupled respiratory complexes I and III, II and III, and the individual complexes IV and V. Further, knockdown reduces ATP levels and causes lactate accumulation (Chen et. al., 2006).

Additionally, hPNPase^{old-35} plays a role in importing small RNAs into the mitochondria, specifically RNase P RNA, MRP RNA, and 5S RNA. RNase P is a ribozyme that cleaves precursor sequences from tRNA molecules. MRP RNA is involved in the initiation of DNA replication in the mitochondria. 5S RNA is a small ribosomal RNA molecule, contributing to the

function of the large ribosomal subunit. hPNPase^{old-35} recognizes these RNAs via a specific stem-loop motif. Importantly, the two roles PNPase plays are not dependent on one another: mutations affecting small RNA import do not affect its RNA processing role (Wang et. al., 2010; Wang et. al., 2011). Figure 2 summarizes the multiple roles PNPase plays in the cell, as well as its multiple locations.

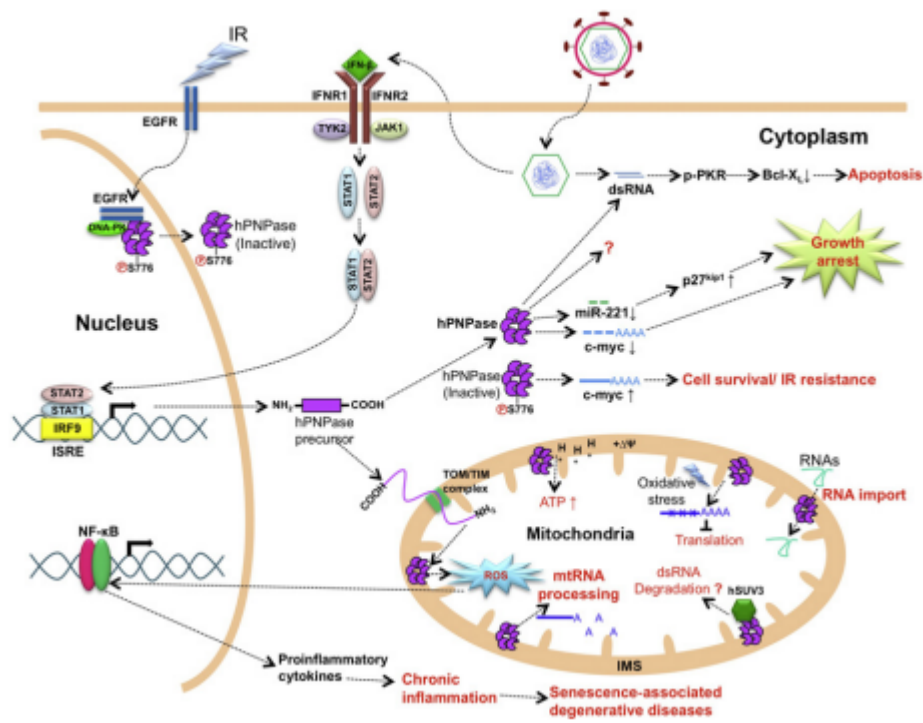


Figure 2: Summary of PNPase roles and subcellular localization. When in the cytoplasm, PNPase is involved in miR-221 and c-myc degradation, leading to growth arrest. PNPase in the mitochondria is involved in mtRNA processing and small RNA import. (Sohki et. al., 2013)

VI. Human Diseases

Recently, PNPase has been shown to be mutated in human hereditary hearing loss (von Ameln et. al., 2012) as well as in a family with myopathy, encephalopathy, and neuropathy (Vedrenne et. al., 2012), both disorders having the hallmarks of mitochondrial disorders. These findings show that PNPase is important in mitochondrial function as well as senescence and terminal differentiation and thus has multiple functional roles. Investigation into one family

revealed that the PNPase mutation resulted in a significant decrease in the 5S rRNA import, underlining its importance in 5S rRNA import into the mitochondria. The affected individuals also had reduced mature MRP-RNA in their mitochondria, though they had normal levels of mtDNA content. Further inquiry into the effect of decreased 5S rRNA import showed a reduction in the amount of COX subunits. This particular family showed the importance of the small RNA import role PNPase plays, and if that is disrupted, the effects it can have on an organism (Vedrenne et. al., 2012). In another family, a different PNPase mutation manifested as hereditary hearing loss. It was determined that there was a decrease in the amount of RNase P imported into the mitochondria of these individuals, and while PNPase was not able to properly homotrimerize it was able to behave as a hypomorph. As there was not the same severity of phenotype as seen in the other family, it is thought that due to the high energy needs of the inner ear, the hypomorph form of PNPase leading to the decrease in small RNA import negatively affected this tissue, though not others. It was further hypothesized that variations in phenotypes will be seen in families with different functional deficits of PNPase, depending on the severity of the mutation (von Ameln et. al., 2012). Cells have multiple mitochondria, and cells requiring a larger energy source, such as muscle cells, having more mitochondria than those that do not require as much energy (mature red blood cells have no mitochondria). Each mitochondria has its own, circular, genome that shows similarity to the genome structure of bacteria, of which there are multiple copies within one mitochondria. The fact that there are variable numbers of mitochondria within cells as well as a variable number of genomes within each mitochondria cause mitochondrial disorders to present with a wide variety of clinical symptoms.

VII. Mitochondria

The mitochondria has long been identified as the location for cellular respiration. This double-membraned organelle is the generator of ATP through the use of a series of respiratory complexes. In addition to playing a role in energy metabolism, mitochondria also play a role in calcium signaling and is closely associated with the endoplasmic reticulum. A certain level of Ca^{2+} is necessary to maintain homeostasis, though if Ca^{2+} levels increase beyond a certain threshold, the mitochondrial membrane potential will collapse, leading to apoptosis (Rizzuto et. al., 2009). In addition to playing a role in Ca^{2+} signaling, mitochondria act as a Ca^{2+} reservoir, with Ca^{2+} being taken up into the matrix (Brighton and Hunt, 1974; Miller, 1998). Mitochondria also play a role in non-calcium evoked apoptosis once the permeability of its membrane has increased due to a variety of apoptotic pathways. The mitochondria will release caspase activators, deactivating proteins which inhibit apoptosis, as well as cytochrome c, which binds to Apaf-1 (apoptotic protease activating factor – 1) (Green, 1998; Fesik and Shi, 2001)

These organelles are not static, but engage in fusion and division in response to cellular conditions. In mammals, three GTPases in the outer membrane, Mfn1, Mfn2, and Opa1, are required for fusion (Martinou and Youle, 2011). Fusion is triggered as a response to cellular stress (Tondera et. al., 2009; Gomes et. al., 2011; Rambold et. al., 2011). Additionally, fusion can rescue mutations within the mitochondrial genome. The rate of fission and fusion changes with differing metabolic demands. Fusion is also enhanced under starvation conditions. Fission is mediated by Drp1, a cytosolic dynamin family member, which forms spirals around the mitochondria which severs both membranes. This process is critical for cells that are growing and dividing, in order to ensure adequate mitochondrial populations in daughter cells. Fission is also used when mitochondria accumulate damage, and can sequester debris on one end of the

mitochondria. Division occurs, and the mitochondria with the debris is autophagocized while the healthy one continues to perform its function in the cell (Youle and van der Bliek, 2012).

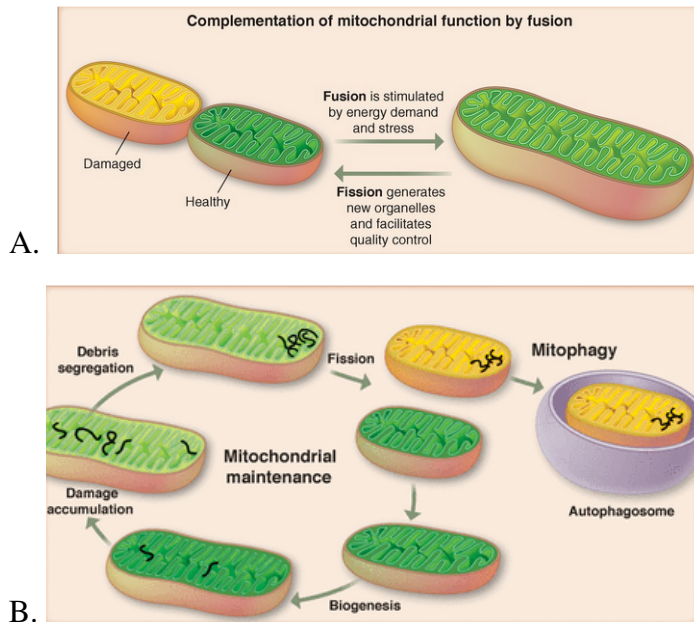


Figure 3: Relation of fusion and fission. The mitochondria in a cell are in a constant flux, and the rate of fission or fusion is dependent on a number of factors, including energy demand, cellular stress, and amount of damage in the mtDNA. (Youle and van der Bliek, 2012)

VIII. *C. elegans*

Caenorhabditis elegans is a free-living soil nematode frequently used as a model organism for a variety of human diseases and processes. The adult worm is approximately 1mm long with 959 somatic cells, and is easily grown in a lab environment on a bacterial lawn. These animals exist mainly as hermaphrodites (XX), though there is a less common male adult (XO) form. Their attractiveness as a model organism exist in their short life cycle of 3 days (Figure 4) and a life span (at 20°C) of around 3 weeks, small, fully sequenced genome, ease of growth, small size, and complete cell lineage mapping. *C. elegans* remains transparent throughout its entire life cycle, enabling cell-level examination via differential interference contrast (DIC) microscopy (www.wormatlas.org). Though anatomically simple, *C. elegans* can be used to study many

complex behaviors such as locomotion, foraging, feeding, defecation, egg laying, sensory responses, mating, social behavior, and learning (Rankin, 2002; de Bono, 2003). However, there are certain drawbacks to using *C. elegans* as a model organism. It is difficult to use molecular techniques to examine the effect of a manipulation on a specific tissue, combined with the fact that worms lack the specialized tissues found in higher organisms such as heart or liver (Van Raamsdonk and Hekimi, 2010).

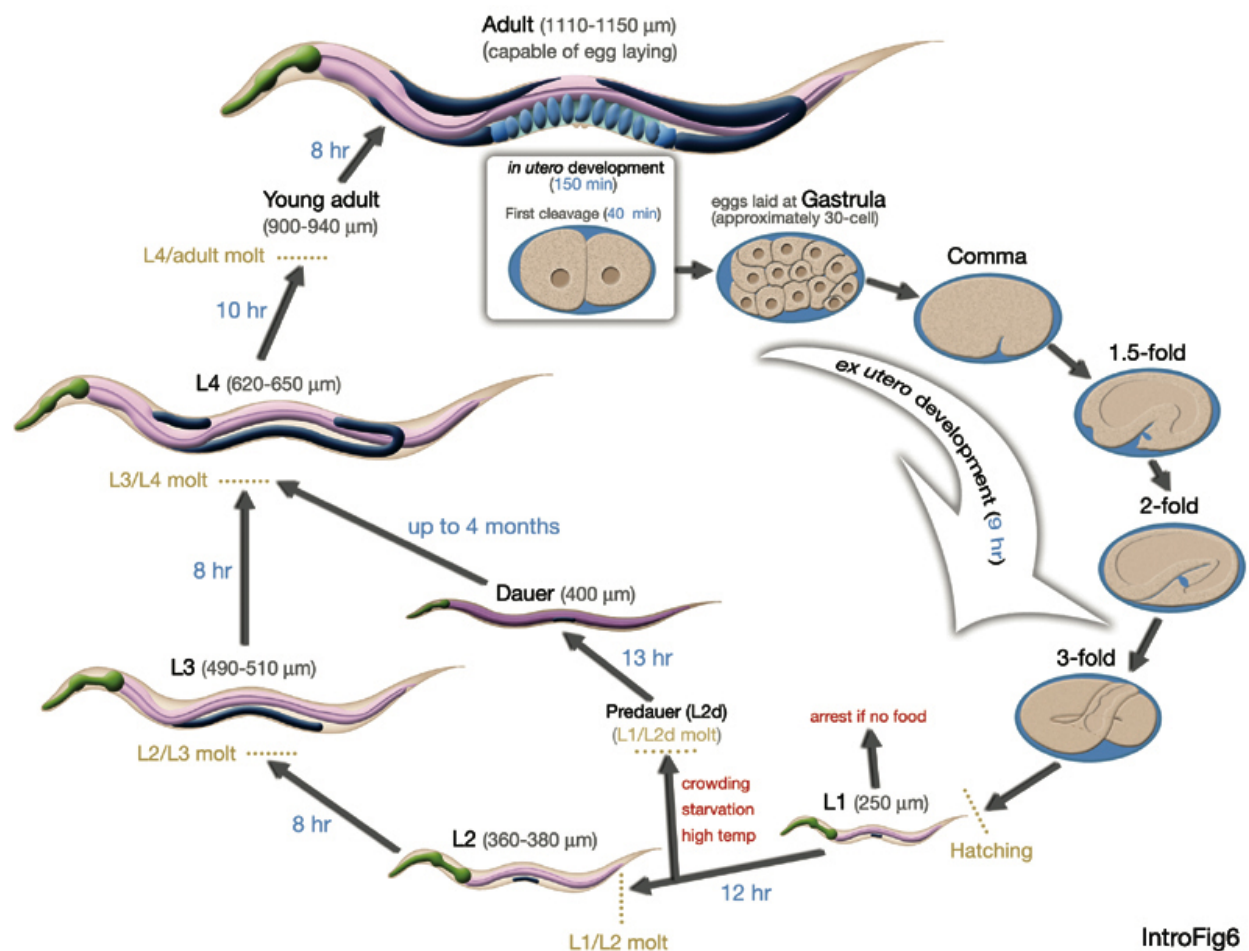


Figure 4: Lifecycle of *C. elegans*. The lifecycle, including time spent in each larval stage as well as the sizes of each stage. Generally, development to adulthood takes 3 days. Eggs mature into the first larval stage, L1, approximately 10 hours after being formed. If there is sufficient food, the L1 animal will proceed into 3 further larval stages: L2, L3, and L4. After the L4 molt,

the young adult will begin to form oocytes. If there is not sufficient food, the L1 larvae will proceed into a dauer stage, which can survive for nearly 4 months without food.

(www.wormatalas.org; Introduction to *C. elegans* Anatomy)

IX. PNPase in *C. elegans*

C. elegans is a versatile model organism that was used for further study of PNPase. There is a worm homolog of PNPT1, BE0003N10.1 (*pnpt-1*), consisting of 10 exons located on chromosome III. This transcript was originally identified during an RNAi profiling of embryogenesis (Sonnichsen et. al., 2005). A deletion mutant (*tm1909*) has also been characterized by a different group, with reported phenotypes of lethality and sterility. However, in this mutant, *pnpt-1* is not the only gene affected. An upstream gene, *chin-1*, is also deleted, thus the gene responsible for the reported phenotypes is unknown. *C. elegans* is particularly attractive model to study gene function due to the ease of knocking down gene expression via RNA interference (RNAi). Given the previous results in mice showing embryonic lethality, knockdown allows for a low level of expression to avoid the lethality seen in other organisms. This is an exciting model of study, as it will give the first *in vivo* look at the knockdown of PNPase in a whole animal system. Pilot studies knocking down PNPase in *C. elegans* identified longevity as an initially identified phenotype.

X. Longevity Pathways

Worms have been used in a number of aging studies, and it has been found that genes or interventions that extend the worm lifespan translate to other organisms, and vice-versa (Van Raamsdonk and Hekimi, 2010). There are a number of known longevity pathways identified in *C. elegans* (Figure 5):

- Disruption of mitochondrial function (Yang and Hekimi, 2010)
- Disruption of translation (Tacutu et. al., 2012)
- Disruption of insulin signaling (Schaffitzel and Hertweck, 2006)
- Caloric restriction (Schaffitzel and Hertweck, 2006)
- Exposure to xenobiotics (Shore, 2012)

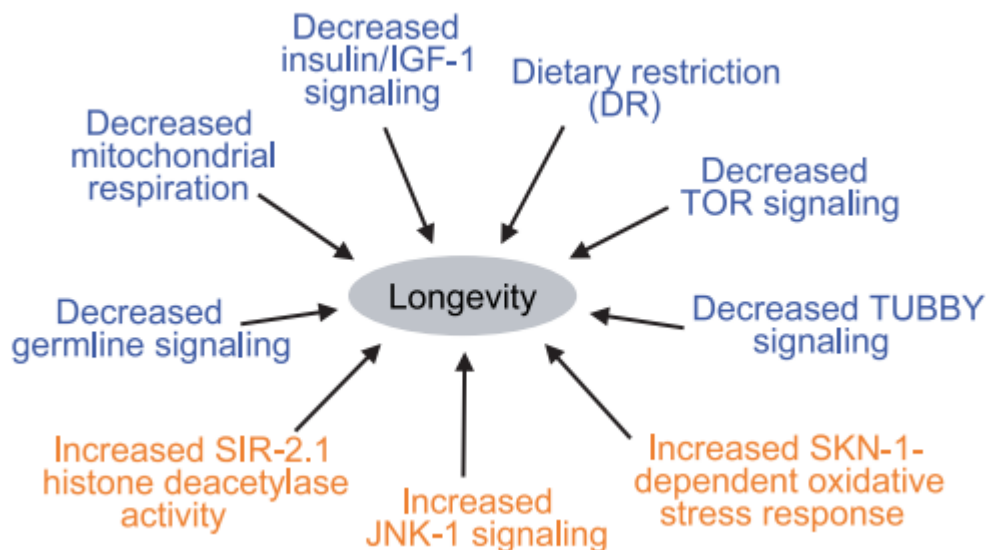


Figure 5: *C. elegans* longevity pathways. Blue indicates decreased activity of the pathway/process while orange indicates increased activity of the pathway/process leading to longevity (Schaffitzel and Hertweck, 2006).

One of the best characterized networks influencing aging is the effect of insulin signaling, specifically the insulin growth factor 1 (IGF-1) system/signaling. Inhibition of this pathway causes constitutive dauer formation (see Figure 4), leading to lifespan extension in adult animals. Animals containing mutations in the IGF-1 pathway show increased fat storage, defective egg-laying, and high tolerance to a variety of stressors (Schaffitzel and Hertweck, 2006; Kenyon, 2005; Kenyon et. al., 1993; Kimura et. al., 1997; Paradis and Ruvkun, 1998).

The mitochondria are the major source of ROS in the cell, and as such, play a role in the length of the lifespan in *C. elegans*. One mechanism to increase lifespan is to detoxify ROS, or to reduce the amount of ROS produced (Schaffitzel and Hertweck, 2006). Another finding is that RNAi targeting of electron transport chain (ETC) complexes during larval development leads to a reduction in oxygen consumption and ATP levels, resulting in a longer lifespan (Dillin et. al., 2002; Lee et. al., 2003). Interestingly, slight increases in ROS have also been found to increase lifespan, likely due to the activation of beneficial stress responses. (Yang and Hekimi, 2010; Schulz et. al., 2007; Zarse et. al., 2012).

Another source of lifespan extension lies in caloric restriction. This mechanism is not specific to *C. elegans*; the lifespan of a number of organisms such as yeast, flies, and rodents can be extended up to 50% by reducing caloric intake (Schaffitzel and Hertweck, 2006). The specific mechanisms, however, are not fully understood and are controversial. Two hypotheses being investigated are that caloric restriction reduces the metabolic rate, and/or that caloric restriction reduces insulin/IGF-1 signaling (Bordone and Guarente, 2005; Walker et. al., 2005).

As a worm ages, there are a variety of physiologic changes that occur, such as decreased pharyngeal pumping, decreased movement, cessation of reproduction, and muscle wasting (Collins et. al., 2008). These changes are also observed in animals with an extended lifespan. It has been shown that mitochondria are critical in energy metabolism, as well as the fact that mitochondrial function declines as an animal ages (Navarro and Boveris, 2007; Shigenaga et. al., 1994). It is possible that the deterioration of the mitochondria as the animal ages helps to cause some of the physiologic changes associated with aging. There are a number of *C. elegans* mutants that are used to study the effect of mitochondrial function on lifespan. *mev-1*, and *gas-1* are two mutants that shorten lifespan when mutated (causing hypersensitivity to oxygen and

superoxides), while *clk-1*, *isp-1*, *lrs-2*, and *nuo-6* extend lifespan when mutated, likely due to a decrease in oxygen consumption, slight overall ROS or the superoxide anion increase, and slower growth (Ishii et. al., 1998; Kayser et. al., 2001; Wong et. al., 1995; Feng et. al., 2001; Lee et. al., 2003; Yang and Hekimi, 2010).

XI. ROS

Reactive Oxygen Species (ROS) are generated when oxygen is reduced, and include hydrogen peroxide, hydroxyl radical, and superoxide. Complex III of the respiratory chain is capable of releasing superoxides into the intermembrane space of the mitochondria. Large increases in ROS can cause damage to proteins, lipids, and DNA. However, a low increase can activate signaling pathways leading to proliferation and transcription (Trachootham et. al., 2008; Droge, 2002; Thannickal and Fanburg, 2000). Cellular respiration is a major source of ROS in cells, and it has been well documented that ROS are upregulated in tumors and can lead to induction of signaling networks causing tumorigenesis and metastasis (Weinberg and Chandel, 2009). A variety of mechanisms exist to counteract the effect of superoxides, namely superoxide dismutases (SODs). SODs convert the superoxide into hydrogen peroxide, which will then be eliminated by a variety of other peroxidases and peroxiredoxins (Sena and Chandel, 2012). Recent studies have shown that a slight increase in ROS, rather than being harmful, will activate beneficial stress responses in animals extending their lifespan (Schulz et. al., 2007; Zarse et. al., 2012).

Chapter 2: Materials and Methods

***C. elegans* culture and maintenance**

C. elegans were grown on NGM plates seeded with 100 uL OP50 bacteria and maintained at 20° C. Worm plates were chunked once a week for strain maintenance or every 3 days to prepare for experiments. For RNAi experiments, the mutant strain CF3152 (*rrf-3* (pk1426)) was used, unless otherwise indicated.

Bleaching of adult *C. elegans*

When plates of worms became contaminated with mold or bacteria, it became necessary to bleach the worms and transfer them to a new plate. A bleach solution was made using 30% bleach and 0.6 N KOH and filter sterilized. On a fresh NGM + OP50 plate, a 20 uL spot of the bleach solution was placed along the edge of the plate. Between 5 and 10 gravid contaminated animals were picked directly into the bleach solution spot. The bleach solution will cause the animals to lay all eggs. Incubate the plate at 20° C, face up, overnight. The following day, L1 larvae are transferred to a new plate.

Generation of RNAi clone

An RNAi clone was generated by amplifying a 558 base pair region 5' of exon 1 to within exon 3 of the wPNPase gene, BE0003N10.1. (wPNPase 5', Ex3 primers, see table 1) from genomic DNA. The fragment was cloned into the EcoRV site of the pBSKS+ vector that had been t-tailed and transformed into DH5 α cells. This fragment was then subcloned into the IPTG-inducible L4440 expression vector using HindIII and XhoI enzymes, and transformed into HT115 cells for use in RNAi experiments.

RNAi

RNAi was distributed via feeding of bacteria expressing dsRNA. dsRNA expression was induced by first growing overnight cultures at 37° C of each bacteria in LB+ampicillin (final concentration of 100 ng/ul). The overnight cultures were then diluted 1:100 in fresh LB+ampicillin (final concentration of 100 ng/ul) and incubated in a 37° C shaker (225 rpm) for 3 hours. IPTG is added to a final concentration of 0.4 mM and returned to the 37° C shaker for 2 hours. Additional ampicillin is added to a final concentration of 100 ng/uL, and a second dose of IPTG is added to a final concentration of 0.4 mM. Plates are then seeded with 100 uL per 6 cm plate or 750 uL per 10 cm plate.

Extracting DNA from *C. elegans*

Adult worms were picked into 20 uL of worm lysis buffer (WLB) with freshly added proteinase K at a concentration of 60 ng/uL. The worm solution was frozen at -80° C for 10-15 minutes, and then incubated at 65° C for 60 minutes. A 15 minute incubation at 95° C is used to inactivate the proteinase K. DNA is stored at -20° C. WLB consists of: 10 mM TRIS (pH 8.0), 50 mM KCl, 2.5 mM MgCl₂, 0.45% Tween 20, 0.45% NP-40, 0.05% gelatin.

Extracting RNA from *C. elegans*

Worms from 15-20 6 cm plates were washed off with M9 and gathered in a 15 mL conical tube. The worms were pelleted at 1000 rpm for 5 minutes, and the supernatant discarded. Worms were washed 3 more times in this manner, using 5 mL M9 for each wash. After the last supernatant was removed, 200 uL Trizol reagent was added. Worms were then freeze-cracked: alternating 20 seconds in liquid nitrogen followed by 1 minute thaw at 37° C, repeated approximately 10 times. The trizol/worm mixture was transferred to a 1.5 mL tube, and 200 uL chloroform added. This was spun at 13,000 rpm at 4° C for 15 minutes. The clear fraction was transferred to a new 1.5 mL tube, and an equal volume of 70% isopropanol was added. The Qiagen RNA prep kit was used from this point forward, following the manufacturer's instructions. RNA was either used for downstream procedures or stored at -80° C.

Generating cDNA from *C. elegans*

In a 0.7 mL tube the following was added: 1 ug RNA, 100 ng oligo primer, 100 ng random primer, and DEPC H₂O to 12 uL. This was incubated at 70° C for 10 minutes. A mix of 1X MMLV RT buffer, 10 mM DTT, 1 mM dNTPs, 10 units RNasein (Promega), and 200 units

MMLV RT was added, and incubated at 37°C for one hour, followed by an incubation at 95°C for 5 minutes. The resulting cDNA was then used for downstream applications or stored at -20°C.

PCR

PCRs were performed with the primers as indicated in Table 1. The PCR was run as follows: 1.5' 94° – [30'' 94° – 30'' annealing temperature – 30'' 72°]x30 – 7' 72°. PCRs were used for verification of primers prior to use in qPCR reactions, to generate RNAi clones, to generate the U6 guide RNA vector for use in CRISPR/Cas9 site directed mutagenesis, and to verify the presence of a mutation. PCRs were run at a total volume of 6.25 uL for verification purposes, and 25 uL when products would be used for downstream purposes, such as cloning or sequencing.

Table 1: Primer sequences and uses

Primer name	Sequence	Notes
U6 F	[GATTAGACCACTTTTACCCGG]GTTTT AGAGCTAGAAATAGCAAGT	[] is guide RNA, rest is U6 vector sequence
U6 R	CAAACATTTAGATTTGCAATTC	Reverse primer to generate guide RNA vector for CRISPR/Cas9
pnpt1 deletion confirmation F	ACCGTCAGCGTCAGCAATTG	To test for mutation from CRISPR/Cas9 site-directed mutagenesis
pnpt1 deletion confirmation R	TTACCTGAGTTTCATAGGAATTT	To test for mutation from CRISPR/Cas9 site-directed mutagenesis
w act-2 F	ATCGTCCTCGACTCTGGAGATG	worm actin; as a loading control
w act-2 R	TCACGTCCAGCCAAGTCAAG	worm actin; as a loading control
fzo-1 F	TTTGTGTCGATGTCCCTGCT	qPCR
fzo-1 R	GAATCGGAACTCGAGGTCTT	qPCR
wPNPase 5'F	AAGTGCCAGCGATCGAGACA	Generating knockdown clone

wPNPase ex3R	CGTTGTCTCCGAATGAAGCA	Generating knockdown clone
COIII R	TATGCATACCTTGAAAGTCT	qPCR testing for polycistronic transcripts
COIII component R	ATAATCACACTACTTCAACA	qPCR testing for total mtDNA
COIII component F	AGACTTTCAAGGTATGCATA	qPCR testing for total mtDNA
ctb-1 F	AAGATGACTAGGTCAATGCA	qPCR testing for polycistronic transcripts
wPNPase ex9 F	ATGATGAATGATGTGCTCGA	qPCR
wPNPase ex10R	GGATTCAGGCTTAGGTGGTT	qPCR

Table 2: Primer pairs and annealing temperature

Primer pair	Annealing temperature (°C)
U6F/U6R	50
pnpt1 deletion confirmation F/R	52
w act-2 F/R	60
fzo-1 F/R	52
ctb-1 F/COIIIR	60
wPNPase ex9F/ex10R	60
wPNPase 5'F/wPNPase ex3R	55
COIII component F/R	57

qPCR

qPCRs were performed at 60° annealing temperature unless otherwise indicated (Table 2). 1X SYBR Green mix (Life Technologies) was used in conjunction with the primers at a final concentration of 0.94 pmol/ul (Table 1) and cDNA diluted 1:16 in a 20 uL single reaction. Reactions were run in triplicate in a 96 well plate, with a standard curve generated for each primer set, with dilutions made at 1:4, 1:8, 1:16, 1:32, and 1:64. Standard curves used control

(L4440) cDNA. This standard curve was then used to generate quantities in the experimental

wells and degree of knockdown calculated via the following equation:
$$\frac{\frac{\text{Avg quantity (knockdown)}}{\text{Avg quantity (control)}}}{\frac{\text{Avg quantity (knockdown actin)}}{\text{Avg quantity (control actin)}}}$$

Egg laying assays

Worms for egg laying assays were age-matched by picking L4 worms onto NGM + carbenicillin plates containing L4440 or Ex3 bacteria and allowed to mature into adults and lay eggs, about 24 hours. The following day, adult worms were removed from the plates and the eggs allowed to mature into adults over the next 3 days. These adults were then used to perform the egg laying assay. One adult worm was picked onto each of ten 2.5 cm NGM + carbenicillin plates. Worms were left on plates for a total of 12 hours, and then removed and eggs counted. A one-way analysis and t-test was performed with the JMP program.

Lifespan Assays

Lifespan assays were performed using CF3152 worms unless otherwise noted, with the indicated bacteria for RNAi. Lifespan assays combining mutant worms with RNAi used MQ887 (*isp-1*; mutation in iron sulfur protein in complex III), MQ1333 (*nuo-6*; mutation in NUDFB4 in complex I), or CB4876 (*clk-1*; mutation in ubiquinone synthesis pathway) strains with the indicated bacteria. Approximately 10 L4 worms were picked onto four 6 cm plates with one of each of the respective bacteria and allowed to mature into adults, and lay eggs; a period lasting 24 hours. The following day, adult worms were removed from the plates, and the eggs allowed to mature into adults. 120 adults were picked onto a large plate and the assay initiated at day 0.

Worms were transferred daily or every other day during the duration of the egg laying period, or approximately 2 weeks. Once the egg-laying period ceased, worms were allowed to remain on the same plate provided sufficient food was present. Worms were considered deceased when a gentle prod with the end of a pick did not cause any movement. If a worm died due to other causes, such as bagging, exploding, or becoming desiccated on the wall, they were considered censored and not included in the statistical analysis. Each experiment was performed with three biological trials. Survival analysis was performed using the JMP program, a Kaplan meier survival curve generated, and the Wilcoxon score used to determine significance.

Adult-initiation Lifespan Assays

Lifespan assays were performed with CF3152 worms that did not develop with RNAi-mediated knockdown. To age-match worms, approximately 10 L4 worms were picked onto four 6 cm NGM plates with OP50 bacteria and allowed to mature into adults, and lay eggs, a period of 24 hours. The following day, adult worms were removed from the plates, and the eggs allowed to mature into adults over the next 3 days. 120 adults were picked onto a large NGM + carbenicillin plate with RNAi bacteria (control L4440 or knockdown Ex3) and the assay initiated at day 0. Lifespan assays were conducted as stated above.

PQ and NAC Lifespan Assays

Paraquat (PQ) plates were prepared by adding PQ to NGM + carbenicillin plates at a final concentration of 0.05 mM. NAC plates were prepared by adding NAC to NGM + carbenicillin plates at a final concentration of 10 mM. Lifespan assays were performed using CF3152 worms,

with the indicated bacteria for RNAi. L4 worms were picked onto four large plates with one of each of the respective bacteria as well as one of each of the plate treatments [L4440 + NGM/carb, L4440 + NGM/carb/PQ, L4440 + NGM/carb/NAC, Ex3 + NGM/carb, Ex3 + NGM/carb/PQ, and Ex3 + NGM/carb/NAC] and allowed to mature into adults, and lay eggs, a period lasting 24 hours. The following day, adult worms were removed from the plates, and the eggs allowed to mature into adults over the following 3 days. 120 adults were picked onto a large plate and the assay initiated at day 0. Lifespans were conducted as previously stated.

ROS Assay

Approximately 10 L4 worms were picked onto control (L4440) or knockdown (Ex3) bacteria and allowed to mature and lay eggs; a period lasting 24 hours. Adults were removed from the plates the next day. Eggs were allowed to mature into adults over the next three days. Plates were washed with M9, and worms were rinsed 3x with M9 to remove bacteria. A 96 well plate was prepared per AmplexRed (Life Technologies) manufacturer's instructions, and approximately 50 adult worms were aliquoted into each well. An absorbance reading was taken at 540 nm, and an average taken. The readings from knockdown and control animals were compared using a t-test.

Visualization of Mitochondrial Network

L4 worms were picked onto control (L4440) or knockdown (Ex3) bacteria and allowed to mature and lay eggs for 24 hours. Adults were removed from the plates the next day. Eggs were allowed to mature into adults over the next 3 days. Mitotracker Red was used to stain live

worms; the stain was diluted according to manufacturer's instructions, and 50 uL aliquoted into microfuge tubes. Twenty live adult worms were picked into each well, and allowed to incubate for 30 minutes at room temperature. Worms were rinsed in M9 before being mounted on a 10% agar pad on a slide. Agar pads were generated by placing a 20 uL drop of liquid agar on a slide and then placing a second slide on top of the drop, flattening it. The second slide was removed after the agar had solidified; usually after one or two minutes. Slides were imaged on an LSM700 confocal microscope at 200X magnification. Mitochondrial networks were quantified using ImageJ software. Microscopy was performed at the VCU Department of Anatomy and Neurobiology Microscopy Facility, supported, in part, with funding from the NIH-NINDS Center core grant (5P30NS047463).

Imaging of Mitochondria

L4 worms were picked onto control (L4440) or knockdown (Ex3) bacteria and allowed to mature and lay eggs. Adults were removed from the plates the next day. Eggs were allowed to mature into adults. Plates were washed with M9 to gather worms, and the worms were washed 3X to remove traces of bacteria. Whole worms were then fixed in 1% paraformaldehyde and 2.5% glutaraldehyde in 0.05 M sodium cacodylate buffer with 0.1 M sucrose for 3-4 days, followed by a post fix of 2% osmium tetroxide in 0.1 M sodium cacodylate buffer, embedded in resin (Embed 812 embedding resin [Electron Microscopy Sciences]), and slices taken for imaging with a TEM. Images showing a cross-section in the pharyngeal region were chosen for further analysis, looking at the size and location of mitochondria, with area measured as the longest axis by the shortest axis. Fixing, resin embedding, and TEM microscopy were performed by the VCU

Department of Anatomy and Neurobiology Microscopy Facility, supported, in part, with funding from the NIH-NINDS Center core grant (5P30NS047463).

NAD⁺/NADH Assay

The BioAssay Systems EnzyChrom NAD⁺/NADH Assay kit was used to measure respiration in *C. elegans*. Whole animals were used in this assay. They were initially freeze-cracked by alternating 20 seconds in liquid nitrogen followed by a 1 minute thaw at 37° C, repeated 10 times. Worms were then homogenized using a pestle in 1.5 mL tubes with appropriate buffers, as recommended by manufacturer's instructions. A calibration curve was also created following manufacturer's instructions. The optical density (OD) was measured at time point 0 and after a 15 minute incubation at room temperature at 565nm. The NAD(H) ratio was calculated using the provided equation: $[NAD(H)] = \frac{\Delta OD_{SAMPLE} - \Delta OD_{BLANK}}{Slope (\mu M^{-1})} \times n (\mu M)$ where n is the dilution factor, if used.

Creation of PNPase mutants

The CRISPR/Cas 9 system was used to create deletions in a targeted area of PNPase. A 20 nucleotide guide RNA sequence was cloned via the Q5 site directed mutagenesis kit (NEB) in a 10 ul reaction into the PU6::unc-119_sgRNA vector (addgene) (see table 1 for primer sequences). The Gibson assembly kit (NEB) was used following manufacturer's instructions to re-circularize the vector. Peft-3::cas9-SV40-NLS::tbb-2 3'UTR (addgene) was used as the Cas9 vector, and mCherry was used as an injection marker. Dr. Laura Mathies performed the

injections into the gonad of N2 wildtype worms. Worms were allowed to recover overnight from the injections, and then individually picked onto NGM + OP50 6 cm plates and their progeny scored. Any L1 larvae that fluoresced were individually picked onto NGM + OP50 6 cm plates and allowed to grow to starvation. An aliquot of these worms was taken for DNA extraction and subsequent sequencing.

Chapter 3: Results

Generation of a PNPase knockdown clone in *C. elegans*

Previous experiments in whole-animal models using PNPase knockout identified it as a gene vital to embryonic development in mice. Later knockout experiments were limited to a targeted liver knockout, which proved to be compatible with life (Wang et. al., 2010). In the *C. elegans* model, an RNAi approach was decided upon (as described in Chapter 2), especially after evaluation of an available deletion mutant demonstrated that two genes were interrupted rather than just PNPase.

An RNAi clone was generated, called Ex3 and spanning the region 5' to exon 1 through exon 3, and evaluated for efficacy in knocking down PNPase. It was found that knockdown animals had an average of 63% reduction of mRNA and a 58% reduction in protein levels (Figure 6).

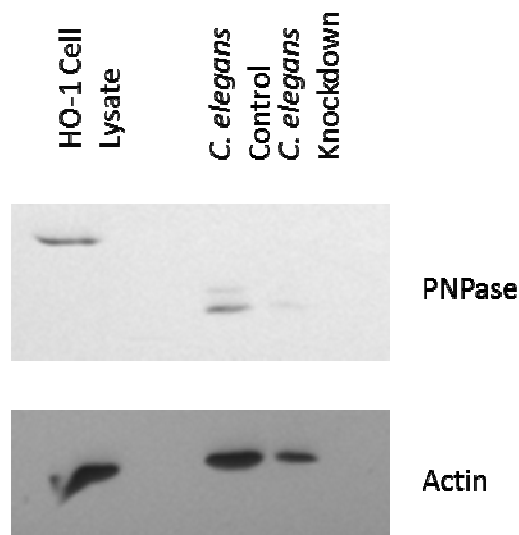
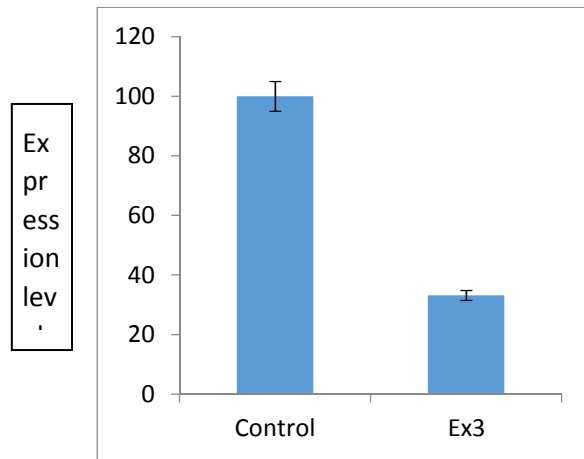


Figure 6: Validation of PNPase knockdown. A. qRT-PCR results indicating an average of 63% knockdown of mRNA. Three biological replicates were performed, and an average taken. B. Western blot indicating a 58% reduction in protein levels. HO-1 cell lysate served as the positive control, and no sample was loaded in the second lane

Characterization of Fertility and Fecundity of PNPase knockdown in *C. elegans*

The deletion mutant had two phenotypes associated with it: lethality and sterility. As knockdown worms were viable and laying eggs, it was unlikely that either of these two phenotypes would be reproduced in this system. However, we did wish to verify that there was not a difference in fecundity in knockdown worms when compared to control. Assays to quantify the number of eggs laid by an animal were also performed to determine if differences in

fecundity is observed. Neither fertility nor fecundity was found to be affected in the knockdown animals (Figure 7).

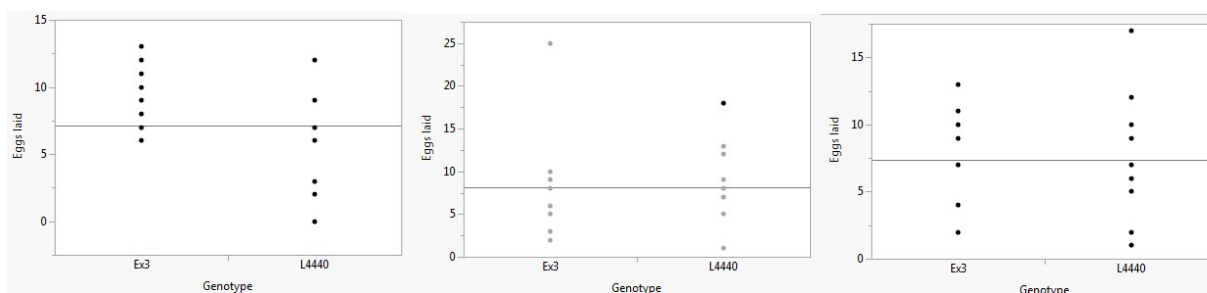
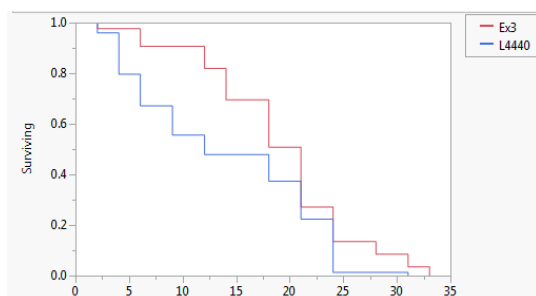


Figure 7: PNPase knockdown does not affect egg laying. Images showing three trials indicating no significant difference in the number of eggs laid between knockdown (Ex3) or control (L4440) animals. Each dot represents egg count of one animal; n=10 for each group in each trial. P-values 0.005, 0.32, 0.31.

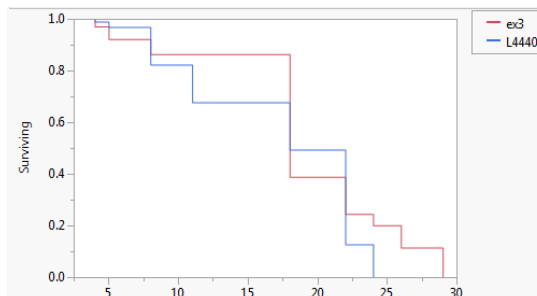
Characterization of Lifespan of PNPase knockdown in *C. elegans*

Further investigation into any potential phenotype associated with PNPase knockdown in *C. elegans* led us to evaluate if knockdown had any effect on the lifespan. As mentioned, there are well characterized mitochondrial mutants that exhibit lifespan extension or reduction. Given the location of PNPase in the mitochondria, we hypothesized that knockdown would affect lifespan. It was found that lifespan in animals with reduced PNPase was modestly but significantly extended (Figure 8, Table 3) Variability in the differences in mean lifespans between each trial are likely due to variability in knockdown efficacy.

A:



B:



C:

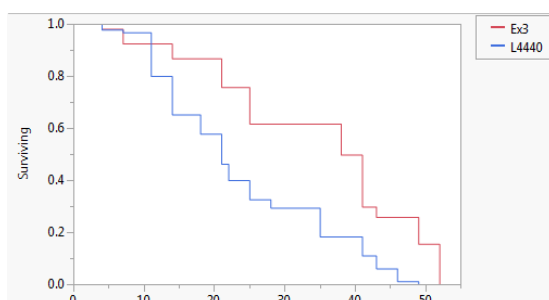


Figure 8: PNPase knockdown extends lifespan in *C. elegans*. A-C are three independent trials of lifespan analyses. Knockdown animals (Ex3) have an increase in lifespan when compared to control animals (L4440)

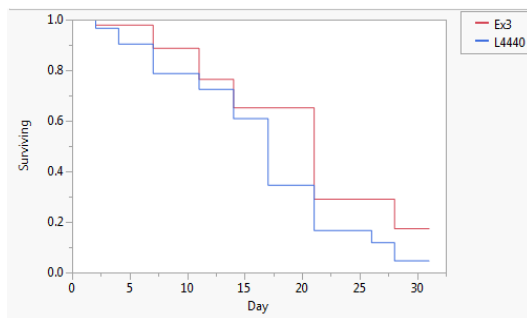
Table 3: Mean lifespans and p-values for trials A-C as seen in Figure 8

Trial	Mean lifespan	p-value
A: L4440	14 days	0.035
A: Ex3	19 days	
B: L4440	17.3 days	0.0092
B: Ex3	19.1 days	
C: L4440	23.8 days	<0.0001
C: Ex3	34.7 days	

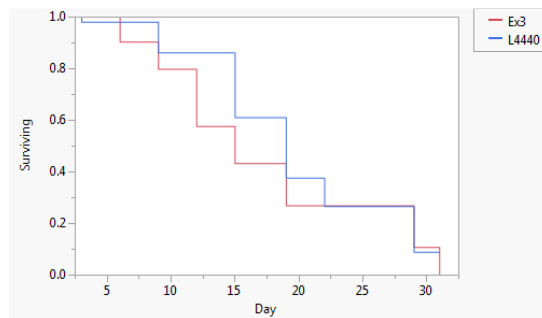
In the initial model, worms were exposed to PNPase knockdown from the time prior to oocyte formation through death. We wanted to determine if this long-term exposure was necessary to

see the lifespan extension effect, or if adult initiation of PNPase knockdown would result in lifespan extension as well. It was determined after multiple trials indicating opposing results or no difference in lifespan that adult initiation of PNPase knockdown show inconsistent results, indicating that to observe consistent lifespan extension with PNPase knockdown, there must be knockdown throughout development (Figure 9, Table 4).

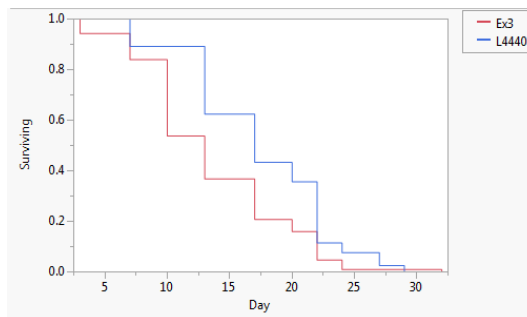
A:



B:



C:



D:

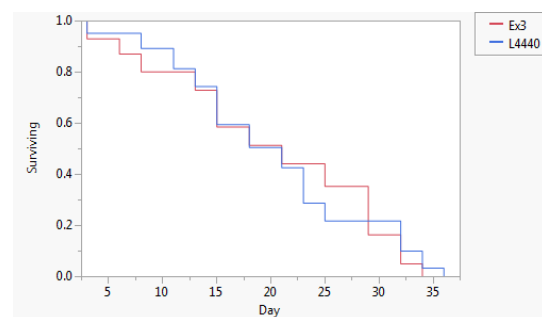


Figure 9: Adult initiation of RNAi produces inconsistent results. Lifespan was extended in control, knockdown, or neither group in different trials.

Table 4: Mean lifespans and p-values for trials A-D in Figure 9.

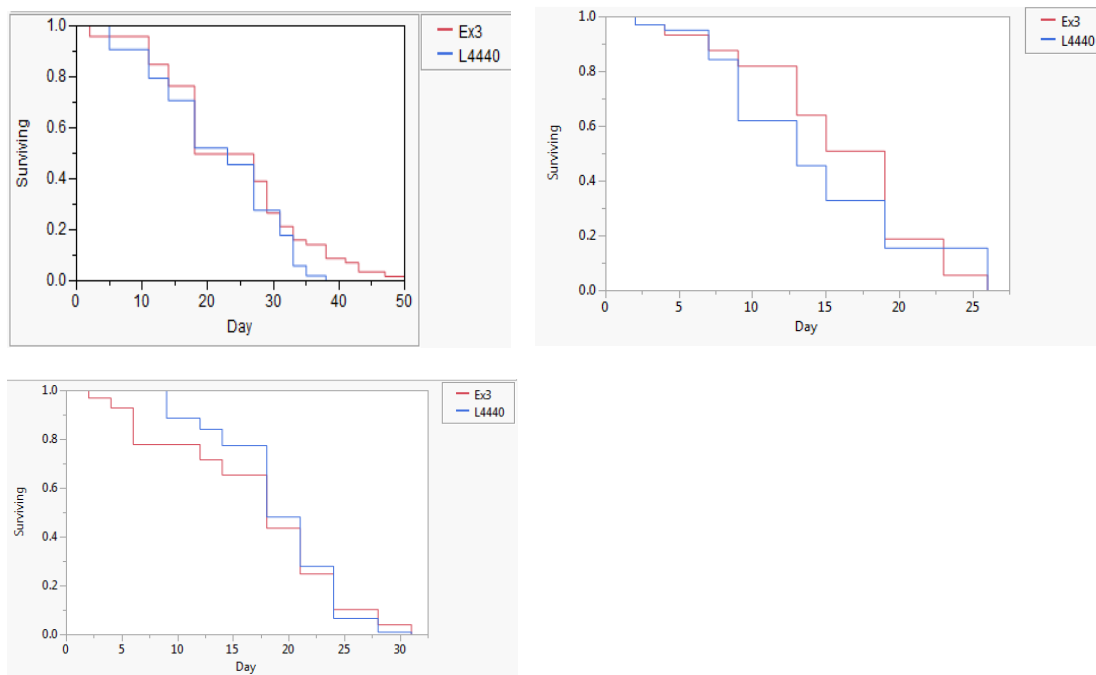
Trial	Mean lifespan	p-value
A: L4440	16.3 days	0.0006
A: Ex3	19.3 days	
B: L4440	19.49 days	0.039
B: Ex3	17.47 days	
C: L4440	17.37 days	<0.0001
C: Ex3	13.4 days	
D: L4440	20 days	0.88
D: Ex3	20 days	

PNPase knockdown acts to extend lifespan in a similar manner as Complex I and Complex III mutants

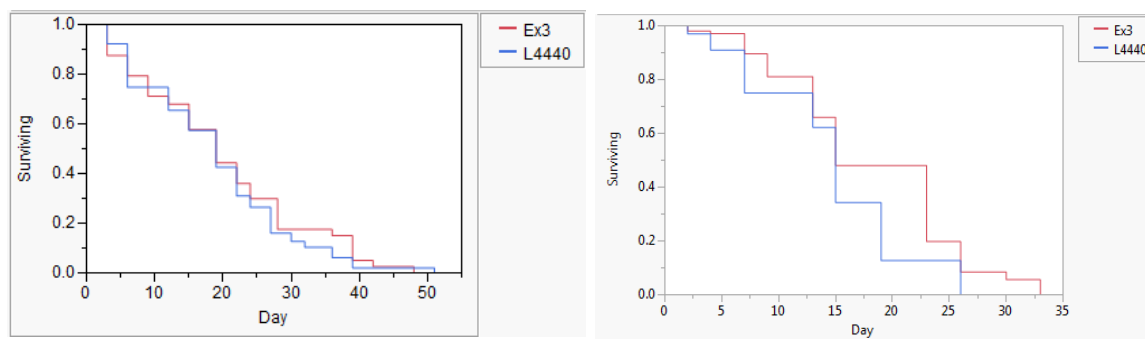
Due to one of the reported locations of PNPase as being the mitochondria, lifespan extension pathways involving the mitochondria were queried. Three previously studied mutants, *nuo-6*, *isp-1*, and *clk-1*, coding for NUDFB4 (a conserved subunit in Complex I), iron sulfur protein in Complex III, and clock abnormal protein 1 encoding the enzyme demethoxyubiquinone monooxygenase, respectively, were fed *pnpt-1* RNAi to create PNPase knockdown animals harboring mutations in genes important in mitochondrial function. If the mutant genes and *pnpt-1* are acting in different lifespan extension pathways, it is expected that there would be further lifespan extension in the mutant/knockdown animals. Conversely, if the mutant genes and *pnpt-1* are acting in the same lifespan extension pathway, it is expected that there will not be any further lifespan extension seen. Lifespan experiments with these animals were performed, and it was found that the combination of the *nuo-6* mutant with *pnpt-1* RNAi and the *isp-1* mutant with *pnpt-1* RNAi did not further extend lifespan. However, the combination of the *clk-1* mutant with *pnpt-1* RNAi did have an extended lifespan when compared to *clk-1* mutant animals fed with vector only bacteria. These results indicate that PNPase knockdown increases lifespan in a

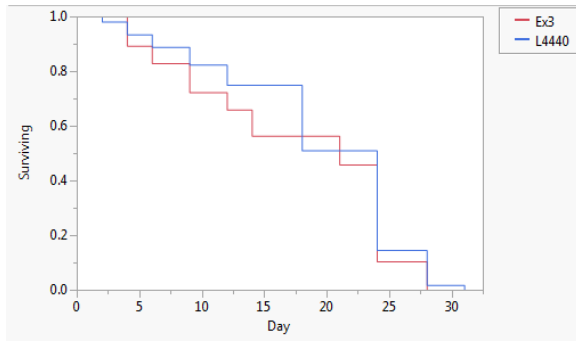
similar manner to the *nuo-6* and *isp-1* mutants but via a different pathway than the *clk-1* mutant (Figure 10, A-C, Tables 5-7).

A:



B:





C:

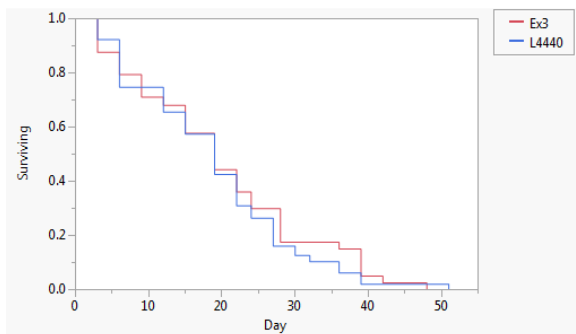
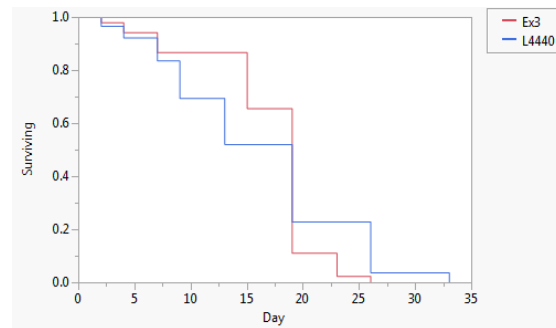
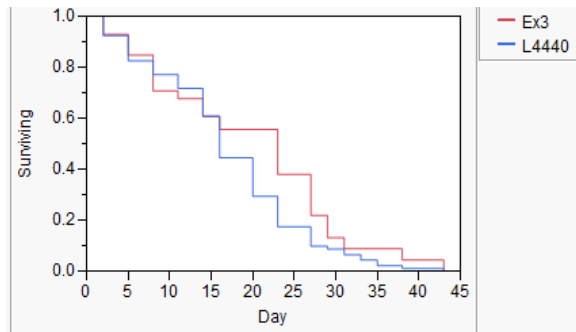


Figure 10: Combining PNPase knockdown with three mitochondrial mutants reveals selectivity in lifespan extension pathway A) *isp-1* mutant animals on RNAi or control bacteria. B) *clk-1* mutant animals on RNAi or control bacteria. C) *nuo-6* mutant animals on RNAi or control bacteria.

Table 5: Mean lifespans and p-values for *isp-1* mutant animals on RNAi or control bacteria, corresponding to Figure 10A

Trial: <i>isp-1</i>	Mean lifespan	p-value
A: L4440	21.7 days	0.18
A: Ex3	23.8 days	
B: L4440	14.3 days	0.28
B: Ex3	16 days	
C: L4440	19 days	0.49
C: Ex3	17.1 days	

Table 6: Mean lifespans and p-values for *clk-1* mutant animals on RNAi or control bacteria, corresponding to Figure 10B

Trial: <i>clk-1</i>	Mean lifespan	p-value
A: L4440	17 days	0.012
A: Ex3	19.64 days	
B: L4440	14.68 days	0.2
B: Ex3	18.1 days	
C: L4440	19.1 days	0.0012
C: Ex3	17.5 days	

Table 7: Mean lifespans and p-values for *nuo-6* mutant animals on RNAi or control bacteria, corresponding to Figure 10C

Trial: <i>nuo-6</i>	Mean lifespan	p-value
A: L4440	18.79 days	0.33
A: Ex3	19.89 days	
B: L4440	16.1 days	0.9
B: Ex3	16.8 days	
C: L4440	18.79 days	0.32
C: Ex3	19.89 days	

PNPase knockdown extends lifespan by increasing ROS

ROS are derived from superoxide, which is generated when oxygen is reduced by one electron.

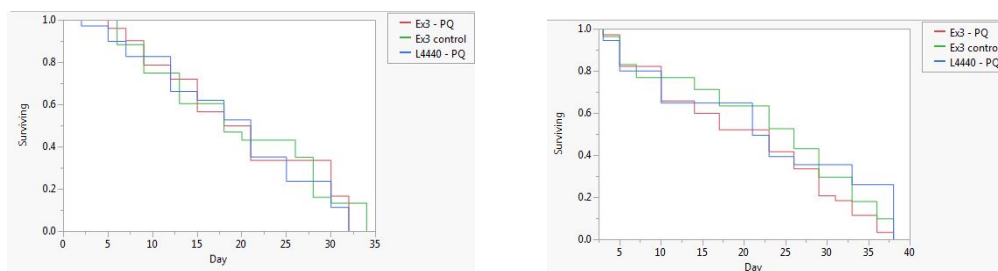
Complex III of the respiratory chain is capable of releasing superoxides into the intermembrane space of the mitochondria. A variety of mechanisms exist to counteract the effect of

superoxides, namely superoxide dismutases (SODs). SODs convert the superoxide into hydrogen peroxide, which will then be eliminated by a variety of other peroxidases and peroxiredoxins (Sena and Chandel, 2012). Recent studies have shown that a slight increase in ROS will activate beneficial stress responses in animals, causing an extension in lifespan (Schulz et al, 2007; Zarse et al., 2012). Mitochondrial mutants, such as *nuo-6* and *isp-1*, exhibit extension in lifespan (Yang and Hekimi, 2010). A mutation in *clk-1*, an enzyme required for synthesis of ubiquinone, has also been shown to extend lifespan, though through an unrelated pathway. *clk-1* animals have enhanced ROS levels, but normal superoxide generation (Yang and Hekimi, 2010).

To determine if PNPase knockdown extends lifespan via an increase in ROS, *pnpt-1* RNAi was used in conjunction with either the superoxide generator paraquat (PQ) or the antioxidant NAC. While the PQ concentration used (0.05mM) was sufficient to extend the lifespan of control animals to that of *pnpt-1* knockdown animals, it did not cause a further extension of lifespan in the *pnpt-1* knockdown animals (Figure 12). This would suggest that the lifespan extension in *pnpt-1* knockdown animals is caused by an increase in superoxides and that additional increase will not cause further increase in lifespan. Alternatively, NAC reduces the amount of ROS. *pnpt-1* knockdown animals in the presence of NAC had a reduction in lifespan to that of the control animals. These results also indicate that ROS plays a role in *pnpt-1* knockdown lifespan extension.

A:

B:



C:

D:

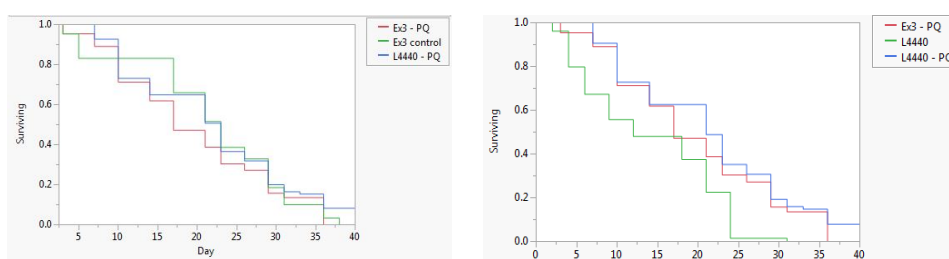


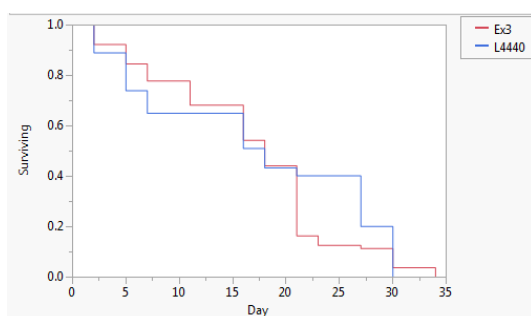
Figure 11: PQ does not further extend lifespan in knockdown animals Lifespans performed with *pnpt-1* RNAi worms and empty vector control on plates containing paraquat (0.05mM). Controls (“Ex3 control” and “L4440” in the figure legends of A-C and “L4440” in D) were grown on NGM plates. D was an additional trial performed to include further controls, and performed only once.

Table 8: Mean lifespans and p-values of worms exposed to paraquat corresponding to Figure 11, A-D

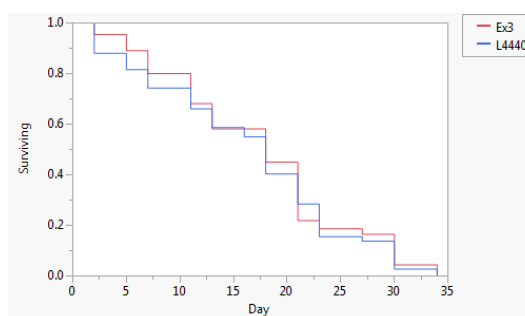
Trial	Mean lifespan	p-value
A: L4440 - PQ	19.1 days	0.53
A: Ex3 - PQ	19.8 days	
A: Ex3 control	19.7 days	
B: L4440 - PQ	22.7 days	0.06
B: Ex3 - PQ	20.1 days	

B: Ex3 control	22 days	
C: L4440 - PQ	21.8 days	0.14
C: Ex3 - PQ	19.5 days	
C: Ex3 control	21.6 days	
D: L4440 -NGM	14 days	<0.0001
D: Ex3 - PQ	19.5 days	
D: L4440 - PQ	21 days	

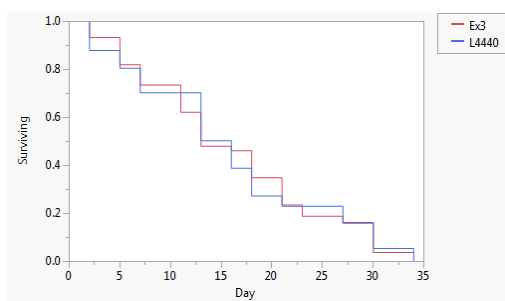
A:



B:



C:



D:

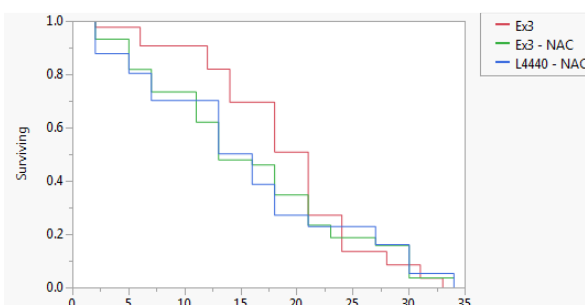


Figure 12: NAC abolishes lifespan extension seen in knockdown animals. Three trials of lifespan performed with *pnpt-1* RNAi worms and empty vector control on plates containing NAC (10mM). Panel D was an additional trial with further controls, and performed only once.

Table 9: Mean lifespans and p-values of worms exposed to NAC corresponding to Figure 12, A-D

Trial	Mean lifespan	p-value
A: L4440	17.3	0.45
A: Ex3	16.7	
B: L4440	16.3	0.54
B: Ex3	17.3	
C: L4440	15.6	0.79
C: Ex3	15.7	

D: L4440	15.6	0.0006
D: Ex3 - NAC	15.7	
D: Ex3-NGM	19	

We wanted to quantify the degree to which knockdown animals had an increase in ROS production, and to determine if it was indeed a measurable amount. The amount of ROS production in the animals was quantified using AmplexRed kit and measuring the ABS of each group (See Chapter 2). It was found that the *pnpt-1* knockdown animals had significantly higher ROS production when compared to control animals, as indicated by a color change and corresponding increase in ABS (Figure 13). This indicates that *pnpt-1* knockdown increases ROS production in a significant amount.

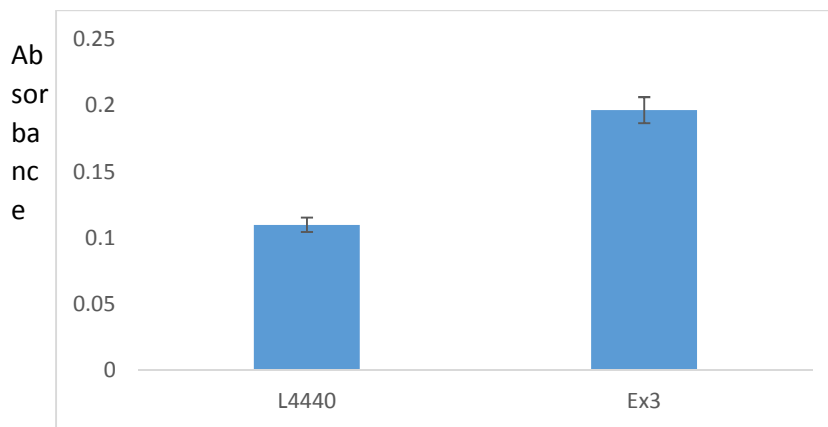


Figure 13: PNPase knockdown increases ROS production. *pnpt-1* knockdown increases ROS production when compared to control over 3 trials. p-value = 0.04

PNPase knockdown affects respiration

To determine if PNPase knockdown has an effect on respiration, as stated in prior knockdown studies, we used the NAD⁺/NADH ratio as a measure of respiration. Using the EnzyChrom

NAD⁺/NADH Assay kit by BioAssay Systems, a ratio of NAD⁺ to NADH was generated in knockdown and control animals, and it was found that knockdown animals had a larger ratio (6.833) than control animals (5.129), indicating more respiration in knockdown animals (Figure 14). However, if the raw data are examined, there is an order of magnitude difference between the knockdown and control animals in the levels of NAD⁺ and NADH, with the reduction seen in knockdown animals. These results are further confounded by the fact that the NAD⁺/NADH ratio and the number and size of the mitochondria are inversely related, unlike our previous mitochondrial data which indicated that knockdown animals have larger or more numerous mitochondria.

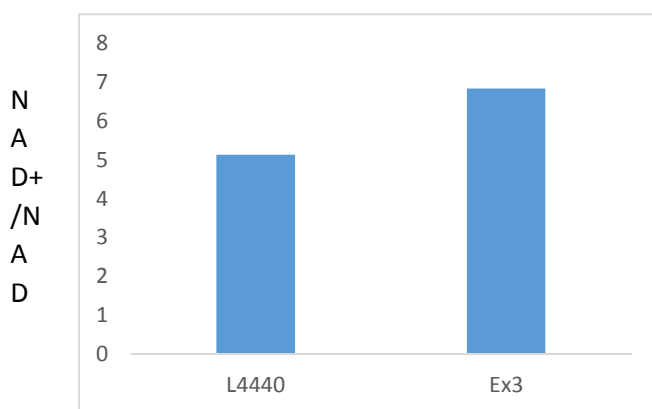


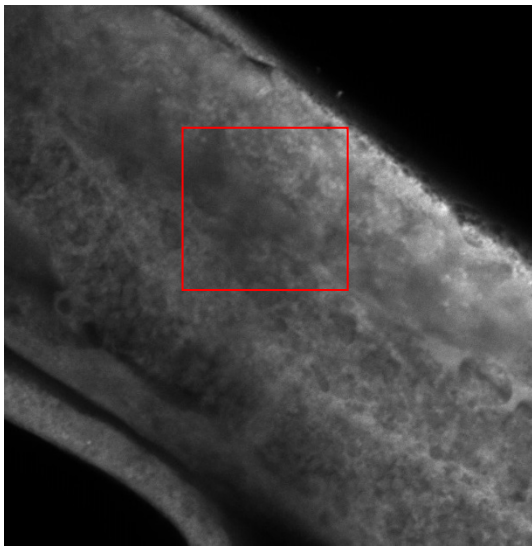
Figure14: PNPase knockdown increases the NAD⁺/NADH ratio. The ratio of NAD⁺/NADH as determined in L4440 control animals was 5.129, compared to Ex3 knockdown animals at 6.833.

PNPase knockdown increases mitochondrial network

To further elucidate the mechanism of lifespan extension and the increase in ROS, we focused on the integrity of mitochondria in these animals. The mitochondrial network was first visualized as a preliminary look at the mitochondria and mitochondrial dynamics. A mitochondrial network is formed as mitochondria divide and fuse, forming an interconnected network. The network

dissolves during apoptosis, which yields numerous small mitochondria (Youle et. al., 2008). Visualization of the mitochondrial network was performed by staining live worms with MitoTracker Red (Figure 15). The network was quantified using ImageJ software and it was observed that *pnpt-1* knockdown animals had a significantly increased network (68.18%) when compared to control animals (38.32%).

A:



B:

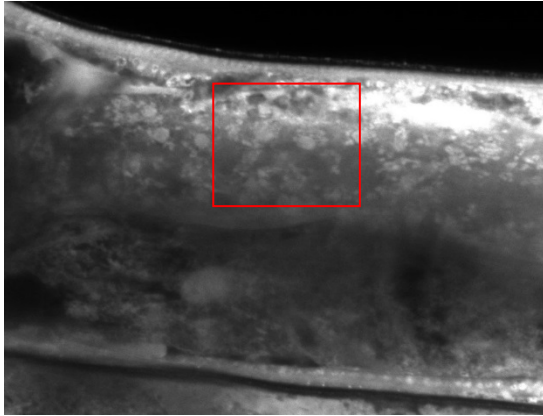


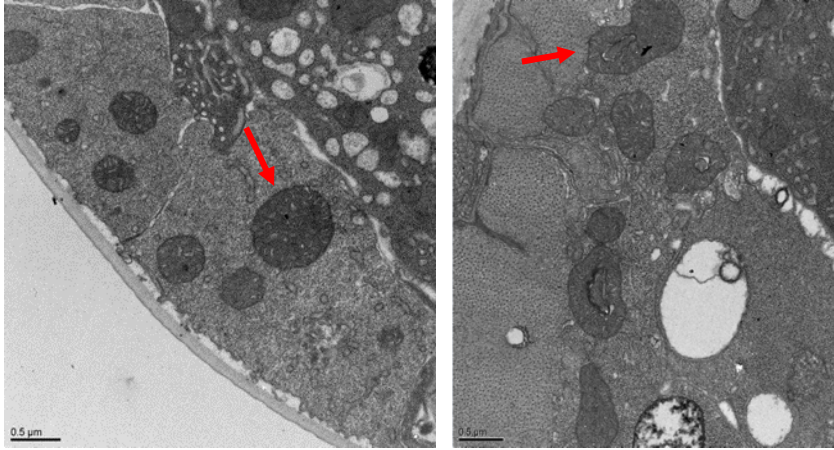
Figure 15: PNPase knockdown increases the mitochondrial network. A & B) Imaging of mitochondrial network via MitoTracker. Control (A) had a network (% of the signal in the ROI that is above threshold) of 38.32% and knockdown (B) had a network of 68.18%, with a p-value of 0.011.

PNPase knockdown does not affect cristae structure

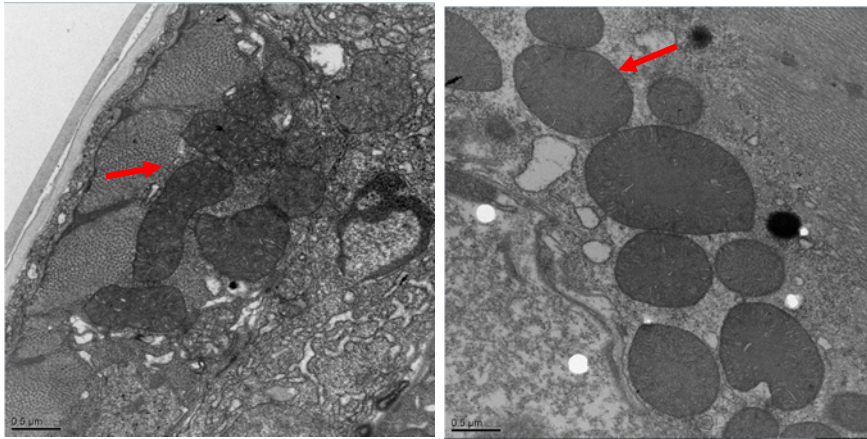
The structure of the mitochondria was also examined in whole animal slices under TEM.

Interestingly, *pnpt-1* knockdown animals had significantly larger mitochondria when compared to control animals (Figure 16 A&B). Mitochondria were measured along the longest and shortest axis, and the average area of control mitochondria was $0.32 \text{ } \mu\text{m}^2$ whereas the average area of knockdown was significantly larger at $0.75 \text{ } \mu\text{m}^2$ (p-value 0.008). The cristae were also examined in the *pnpt-1* knockdown animals and it was determined that there was no observable difference in the cristae structure or organization when compared to control animals (Figure 16 C&D).

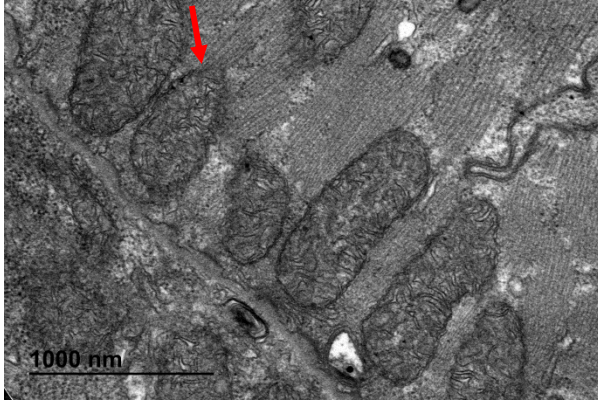
A: Images from control animals



B: Images from knockdown animals



C:



D:

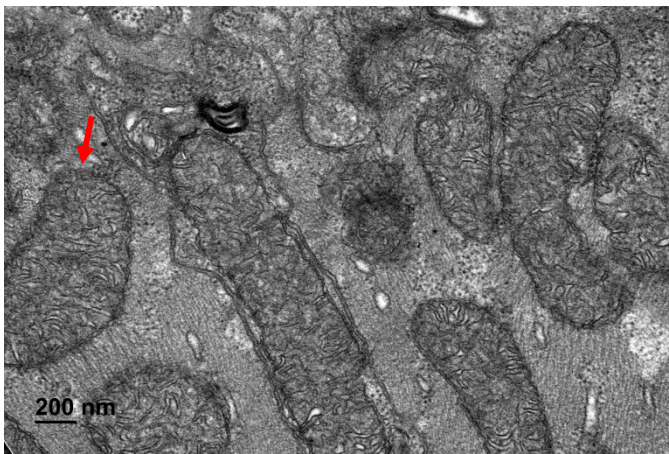


Figure 16: Knockdown affects mitochondria size but not cristae structure A & B) TEM images of mitochondria from control (A) and knockdown animals (B), 10000X. Knockdown animals had significantly larger mitochondria, p-value 0.008. C & D) TEM images of mitochondria from control (C) and knockdown (D) animals, 60000X. Examination of the cristae did not show any difference. Red arrows indicate mitochondria.

PNPase knockdown increases the amount of polycistronic mitochondrial transcripts

The mitochondrial genome is a circular piece of DNA that is transcribed in one long polycistronic transcript and later processing is necessary to separate individual RNAs (Figure 17). RNase P is one enzyme responsible for this processing, specifically the excising of intervening tRNAs. As PNPase is involved in the import of RNase P RNA, we wanted to investigate if there was an effect on the mitochondrial transcript in knockdown animals. The

amount of polycistronic transcripts was quantified at the junction of *ctb-1* and COIII. The amount of polycistronic transcript and total transcript was determined via qPCR, and it was found that there was 66 times more polycistronic transcripts in the knockdown animals when compared to control, indicating that the mitochondrial transcript is not being properly spliced (Figure 18).

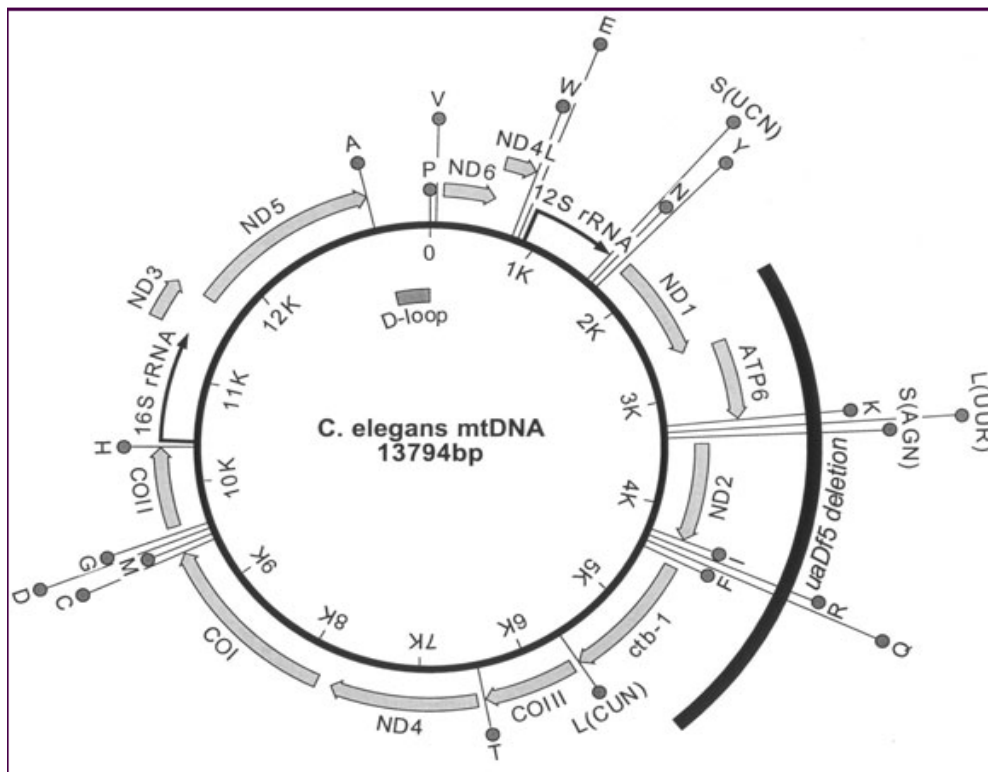


Figure 17: Locations of genes and tRNAs in the *C. elegans* mitochondrial genome. The *C. elegans* mitochondrial genome, indicating the locations of genes as well as intervening tRNAs (bubbles). The mitochondrial genes are transcribed as a polycistronic transcript and later cut. (www.wormbook.org)

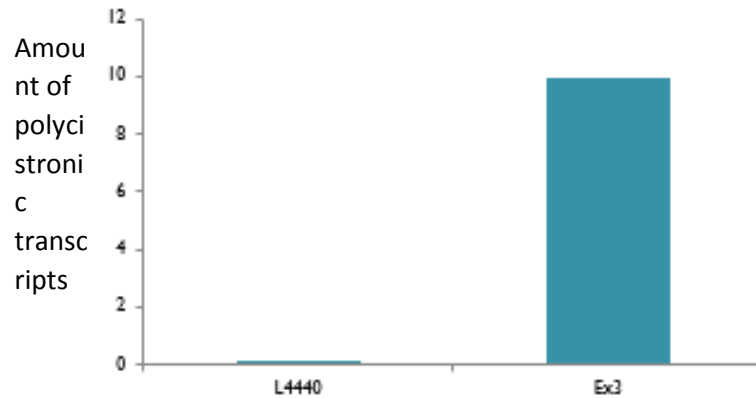


Figure 18: PNPase knockdown increases polycistronic transcripts. Knockdown(Ex3) animals have 66 times more polycistronic transcripts when compared to control (L4440). The graph represents a single trial.

PNPase knockdown increases *fzo-1*

Another target of ROS are the mitochondrial fusion proteins mfn 1 and mfn 2 in humans. An increase in ROS increases the expression of these proteins, leading to an increase in mitochondrial fusion. mfn2, mitofusion-2, is a GTPase located in the outer membrane of the mitochondria that, along with mfn1, is essential for mitochondrial fusion. Mouse cells lacking mfn1 and 2 showed a decrease in membrane potential as well as a reduced oxidative phosphorylation (OXPHOS) (Chen et. al., 2005). Levels of *fzo-1* mRNA, the worm homolog of mfn2, were evaluated to determine if knockdown of PNPase was increasing *fzo-1* expression and potentially linking the increase in ROS to the increase in mitochondrial size. An increase in mitochondrial fusion would cause larger mitochondria. Investigation into *fzo-1* showed that there was an increase in the amount of transcript in knockdown animals (Figure 19).

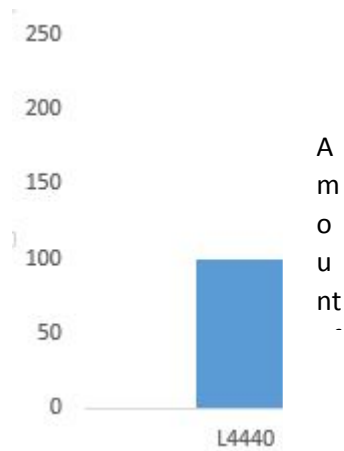


Figure 19: PNPase knockdown increases *fzo-1* expression. *fzo-1* expression is increased two-fold in knockdown (Ex3) animals when compared to control (L4440). The graph represents a single trial.

Generation of PNPase mutant strains

The CRISPR/Cas9 system was used to generate targeted deletions in PNPase (see Table 1 for primer sequences). Of 14 injected worms, 9 individual strains were recovered that had the potential for carrying the mutation. These were sent for sequencing, and it was determined that 3 strains had single base pair deletions, two of which (6 and 9) resulted in a frameshift and a premature stop codon. Strain two had a single base pair deletion resulting in a frameshift mutation and early stop codon. Two strains (strain 6 and 9) had identical deletions while strain 2 had a different deletion (Figure 20).

Stop codon located 15 amino acids downstream

R R E L S H L T M K S S S P E P L T G

Clones 6 and 9: G[CGT][CGT][GAG][CTC][AGT][C-AT][CTG][ACA][ATG][AAA][TCC][TCA][TCT][CCA][GAG][CCA][TTG][ACA][GGT]

Wild type: G[CGT][CGT][GAG][CTC][AGT][CAA][TCT][GAC][AAT][GAA][ATC][CTC][ATC][TCC][AGA][GCC][ATT][GAC][AGG]T

R R E L S Q S D N E I L I S R A I D R

Stop codon located 15 amino acids downstream

R R E L S Q S D M K S S S P E P L T G

Clone 2: G[CGT][CGT][GAG][CTC][AGT][CAA][TCT][GAC][ATG][AAA][TCC][TCA][TCT][CCA][GAG][CCA][TTG][ACA][GGT]

Wild type: G[CGT][CGT][GAG][CTC][AGT][CAA][TCT][GAC][AAT][GAA][ATC][CTC][ATC][TCC][AGA][GCC][ATT][GAC][AGG]T

R R E L S Q S D N E I L I S R A I D R

Figure 20: Deletion strains. Clones 6 and 9 had identical deletions, resulting in a frameshift and early stop codon. Clone 2 had a different deletion, also resulting in a frameshift seven nucleotides 3' of the clone 6 and 9 deletion and an early stop codon.

Overall, we determined that knocking down PNPase in the *C. elegans* model is not lethal, leading to the creation of a whole-animal model that allows for systemic characterization of PNPase knockdown. We determined that knockdown increases lifespan via an increase in ROS production. Additionally, we quantified the amount of ROS being produced by the knockdown animals. Investigation into mitochondrial networks and morphology showed that knockdown animals have an increased mitochondrial network as well as larger mitochondria. However, we did not find that knockdown animals had disordered cristae, as has been reported in other organisms. Interestingly, we found that the NAD⁺/NADH ratio is higher in knockdown animals, which would seem to conflict with our other results. This finding needs to be further investigated. We further looked into the possibility of accumulation of polycistronic transcripts in the mitochondria as a result of decreased RNase P import, and found that there was a large

increase in the amount of polycistronic transcripts in knockdown animals. Moreover, we found that there was an increase in the amount of *fzo-1*, a ROS-induced protein responsible for mitochondrial fusion, and potentially linking PNPase knockdown with the increased mitochondrial size observed.

Chapter 4: Discussion

PNPase knockdown in *C. elegans* increases lifespan

This study was undertaken in an attempt to determine the effect of knocking down PNPase on a whole animal. Previous experiments performed in mice proved that a whole animal knockout was embryonic lethal, indicating that PNPase was necessary during the course of mammalian development (Wang et. al., 2010). Using *C. elegans* allowed us to use RNAi to knockdown the gene, still allowing for a low level of expression in the event that PNPase was also necessary to development in lower organisms. Confirming our results with a deletion mutant would answer the question of whether PNPase is necessary for *C. elegans* development. Additionally, the use of a deletion mutant will aid in eliminating the variability in lifespan extension seen in the knockdown model, with differences in means ranging from 2 to 11 days. During the course of our investigation into phenotypes created by knocking down this enzyme in *C. elegans*, it was discovered that knockdown significantly extends lifespan when the knockdown is present starting at oocyte formation. However, only initiating knockdown once animals reach adulthood was not sufficient to cause a repeatable phenotype. Adult-initiation lifespans showed a wide variety in results, indicating the probability that initiating knockdown only during adulthood does not produce consistent effects as well as indicating the likelihood that the mechanism causing the increase in lifespan is present starting at an early stage in development. Further investigation into exact timing of knockdown may prove to be insightful,

as it would help determine exactly at what point in development knockdown has to be present from in order to cause lifespan extension.

Of further interest in this lifespan extension would be an investigation into miRNA levels. miRNAs that are traditionally degraded by PNPase would have higher levels in the knockdown model, and may also play a role in the lifespan extension observed. Investigating miRNA levels via a microarray may lead to targets to investigate.

PNPase knockdown increases ROS production

To determine the potential cause of lifespan extension, we utilized three mitochondrial mutants in combination with knockdown RNAi. Due to one of the locations of PNPase being reported as the mitochondria, we focused on lifespan extension pathways involving mitochondrial mutants. In previous studies, *nuo-6* and *isp-1* mutants have increased superoxide anion generation but not an increase in overall ROS whereas *clk-1* mutants have an increase in overall ROS but not the superoxide anion. In the *nuo-6* and *isp-1* mutants, it is thought that the increase in superoxide can trigger mechanisms that slow down aging at the level of gene expression. Alternatively, the lifespan extension of the *clk-1* mutants is not entirely worked out. *clk-1* mutants have impaired ubiquinone synthesis, which can affect a variety of cellular processes, as ubiquinone is found in all membranes as well as being a pro-oxidant and an anti-oxidant (Yang and Hekimi, 2010).

Additionally, application of NAC, an anti-oxidant on all types of ROS, abolishes lifespan extension seen in *nuo-6* and *isp-1* mutants but has no effect on the extension seen in *clk-1* mutants, indicating that ROS metabolism is not important to the increased lifespan in *clk-1*

mutant animals, as even in the presence of NAC their lifespan remains increased. Further, PQ application significantly extended the lifespan of *clk-1* mutant animals while not affecting that of *nuo-6* and *isp-1* animals, underlining the difference in superoxide levels between the two groups (Yang and Hekimi, 2010).

It was found that the lifespan extension in PNPase knockdown animals modeled that of *nuo-6* and *isp-1* mutants, indicating a probable OXPHOS and/or superoxide production link. It did not, however, follow the same pattern as the *clk-1* mutant, which, given its different behavior from that of the other mutants, is not surprising. This is a novel phenotype associated with this gene, and is worthy of further investigation.

To delve further into the ROS production question, we used the superoxide generator paraquat (PQ) as well as the antioxidant NAC to determine if combining these with PNPase knockdown would have any effect on the lifespan extension being observed. It was determined that the presence of PQ did not cause any further extension of lifespan in knockdown animals, though it was shown to increase the lifespan of control animals. Additionally, application of NAC reduced the lifespan of knockdown animals to that of control animals, while having no effect on control animals.

Additionally, the amount of ROS produced by knockdown and control animals was quantified, in order to determine the degree to which ROS, specifically superoxide, was increased in knockdown animals and it was found that knockdown animals were producing nearly 50% more superoxide than control animals. The assay used measured superoxides via its conversion to hydrogen peroxide. Combining these two results, it is probable that the lifespan extension seen in knockdown animals is being caused, at least in part, by an increase in superoxide production. While it has generally been held that an increase in ROS is detrimental

to an organism, recent studies have shown that a slight increase in ROS, rather than being harmful, will activate beneficial stress responses in animals extending their lifespan (Schulz et. al., 2007; Zarse et. al., 2012). This appears to be happening in knockdown animals, as lifespan extension is being caused by an increase in superoxide. Measuring the overall ROS would also be informative, as there are many types of ROS in cells. If one type of ROS is being increased, but there is not an overall increase in ROS, then that would indicate other types of ROS are being simultaneously decreased. However, if there is an overall increase in ROS, then there is no compensation for the increase of one type. In our model, there is an increase in superoxide. I would expect that there is not an increase in overall ROS in our model, indicating that other types of ROS would be decreased.

Of interest would be to determine if increasing other ROS will also cause an increase in lifespan, or if the increase being seen is due solely to superoxide increase. Exposing animals to other common ROS, including hydrogen peroxide, hydroxyl radicals, peroxide, and hydroxyl ions, will identify if other ROS are able to increase lifespan in a similar manner as superoxide.

Further investigation into the stress responses of *C. elegans* may help to link knockdown, increase in ROS, and extended lifespan. Knockdown of PNPase could be causing a stress response in *C. elegans*, which in turn is triggering the increase in ROS and subsequent lifespan extension. Of particular interest would be the effect of PNPase knockdown on the oxidative stress pathway, with the measurement of dopamine levels an indicator. High levels of ROS trigger the oxidative stress pathway, and it has been shown that ROS induction can lead to reduced dopamine levels (Rodriguez et. al., 2013). Another pathway of interest would be the hypoxic stress pathway, which has also been associated with oxidative stress. Measuring the

levels of HIF-1 would indicate whether or not this pathway is being activated as a response to PNPase knockdown (Rodriguez et. al., 2013).

PNPase knockdown increases the NAD⁺/NADH ratio

To investigate the effect of PNPase knockdown on respiration, we measured the NAD⁺/NADH ratio and found that knockdown animals actually had a higher ratio when compared to control animals. While the NAD⁺/NADH ratio can be affected at different points in the reaction pathway (changing pyruvate to lactate, for example), of immediate relevancy is the fact that Complex I of the respiratory chain is where NADH is reduced to NAD⁺. This is one of the complexes examined in this study, with the use of the *nuo-6* mutant. Interestingly, an elevated NAD⁺/NADH ratio has been found to decrease mitochondrial content, increase autophagy, and induce mitochondrial fragmentation (Jang et. al., 2012). NAD⁺ also activates SIRT1, which may promote cell cycle progression and longevity (Giannakou et. al., 2004).

Our results seem to be in opposition to our other findings, as the NAD⁺/NADH ratio is inversely related to mitochondrial number and size. We have found that knockdown animals have increased mitochondria and a greater mitochondrial network, yet are also showing an increased NAD⁺/NADH ratio. Combining these data will require further investigation to paint a complete picture. However, if the absolute numbers are investigated, we find an order of magnitude difference between the knockdown and control in the levels of NAD⁺ and NADH (NADH levels of 0.71 in the control compared to 0.069 in the knockdown, for example), a great reduction observed in knockdown animals. This, too, may be worthy of further investigation, as the ratio itself may not be telling the full story and the absolute amount of respiration may affect

mitochondria function and its effect on lifespan. Additionally, being able to directly measure respiration via a Clark electrode, which measures mitochondrial oxygen consumption, would be beneficial to further evaluate this data.

PNPase knockdown affects mitochondrial network, morphology, and distribution

Prior work done in *C. elegans* has indicated that mitochondrial defects result in a denser mitochondrial network (Lee et. al., 2003). We tested the mitochondrial network, as well as imaging the individual mitochondria of knockdown animals and found that there was an increase in network in the knockdown animals when compared to control. Further, knockdown animals had larger mitochondria when compared to the control animals, indicating a possible dysregulation of the fusion/fission rate of the mitochondria. *fzo-1*, the worm homolog of mfn-2, is upregulated by ROS, causing increased mitochondrial fusion (Robb et. al., 2013). Our findings of increased *fzo-1* indicate a potential mechanism for the observed increase in mitochondrial network and dysmorphic mitochondria.

Mitochondria are constantly dividing and fusing together, which help to fine-tune cellular processes including ROS and ATP production (Archer, 2013). Fusion has also been shown to assist in alleviating cellular stress by causing the contents of damaged and undamaged mitochondria to mix (Youle, 2012). Given the findings of filamentous and granular mitochondria, a decrease in membrane potential, and a decrease in the enzymatic activity of the respiratory complexes in HEK-293T cells as well as our findings of an increase in ROS production, an increase in the fusion rate may be expected in knockdown animals as a way of attempting to relieve the cellular stress caused by these alterations (Chen et al., 2006). Further,

there is a growing body of evidence implicating disordered mitochondrial dynamics can contribute to complex diseases, including cancer and neurodegeneration. Cancer cells have shown increased mitochondrial fragmentation, implicating the protein responsible for fission, drp1, as a potential cancer biomarker. Investigation into heritable neurodegenerative conditions indicates that an increase in the fission rate, and a corresponding decrease in the fusion rate, can be harmful to neurons. Heritable juvenile parkinsonism, for example, has a mutation in the PINK1-parkin pathway, which normally functions to reduce mitochondrial oxidative stress, prevent fission, maintain membrane potential, and maintain a fused mitochondrial network (Archer, 2013).

While knockdown of PNPase has not yet been associated with a cancer phenotype, mutations in the gene in humans cause phenotypes mirroring that of mitochondrial disorders, which come with a complex set of presentations, neuropathy and hearing loss among them. Research into both these families has underscored the importance of PNPase in the import of small RNAs in mitochondrial function, though it may be interesting to investigate the mitochondrial dynamics of these individuals to determine if there is any additional mechanistic explanations (Vedrenne et. al., 2012; Ameln et. al., 2012).

PNPase knockdown increases mitochondrial polycistronic transcript accumulation

The downstream effects that knockdown of PNPase has, such as an increase in ROS, and the effect it has on mitochondrial fusion, can indicate potential therapeutic targets not only for the human disease associated with PNPT1 mutation but also cancer. We also showed that PNPase knockdown causes an accumulation of polycistronic transcripts in the mitochondria.

This has two implications, either or both of which may play a role in the increase in ROS, and consequently the increase in lifespan, in knockdown animals. First, an accumulation of polycistronic transcripts is rendering unavailable a number of mitochondrial-encoded subunits of the respiratory complexes, affecting each one with the exception of Complex II. This could affect the availability of subunits to form respiratory complexes, and therefore causing the complexes to “leak” ROS as well as affecting their efficiency resulting in the decrease in membrane potential seen previously (Chen et. al., 2006).

A western blot can be used to quantify the components in the respiratory complexes. Specific antibodies would be necessary, and while this would not tell if the complexes themselves are being formed properly, it will be possible to determine if less RNA corresponds to less protein. Further, to determine if a decrease in respiratory complexes is interrupting respiration, the mutants *nuo-6* (Complex I mutation) and *isp-1* (Complex III mutation) can be used. Measuring the respiration in these mutants would show the effect these mutations have on respiration.

A second implication is that the tRNAs are also not being excised resulting in less tRNAs available for protein translation. This lack of available tRNAs may lead to fewer mitochondrial proteins being translated, among them subunits of the respiratory complexes. As a lack of tRNAs would affect more than just the subunits of the respiratory complexes, and have a broader effect, this may explain why knockdown not only causes a decrease in membrane potential, but also dysmorphic mitochondria. Teasing apart these two possibilities would be worthy of further investigation, though it is likely that they both contribute to the phenotypes being observed in knockdown studies.

Conclusions

Our studies have shown that a decrease in the amount of PNPase causes an increase in lifespan via increased ROS production. We have also shown that knockdown causes alteration in the fission/fusion ratio of the mitochondria, though we did not find disordered cristae reported by other groups. It is possible that this is due to the fact that we are looking in the whole animal as opposed to cells, allowing for the action of other pathways and recovery mechanisms.

Further studies are required to fully elucidate the mechanism of increased ROS production in knockdown animals, as well as the impact of the reduction in respiratory chain subunits. It would be interesting to determine if the subunits are being formed properly in lower numbers, or if they are unable to be formed. One way to approach this would be via a western blot analysis, with appropriate, specific antibodies. This would give information on the ratio of the subunits, as well as relative subunit levels across groups. To specifically determine subunit structure, protein crystallization would need to be carried out on extracted mitochondria. Further, determining if the accumulation of polycistronic transcripts is causing ROS to “leak” or if ROS levels are increased as a stress response would be enlightening. Looking into levels of dopamine and HIF-1 would help to determine if animals are exhibiting an oxidative and/or hypoxic stress response. Combining these insights with those gained by determining if appropriate levels of the respiratory complex subunits are being formed will help further the understanding of these phenotypes. Further studies can be done on *C. elegans* PNPase mutants generated via the CRISPR/Cas9 system. These mutants will allow for studies to be performed where there is no PNPase, or where PNPase is truncated. This would be in contrast to the knockdown studies, where there is full-length PNPase present, though at lower levels than in

wild-type animals. These insights can provide further information to the causes and suggest potential treatments for the human mitochondrial disorders caused by mutations in *pnpt1*. The *C. elegans* model would additionally be an attractive model for initial testing of genetic therapies for these human mitochondrial disorders, though further investigations would need to be performed in higher organisms.

Given all our data, the following hypothetical model (Figure 21) has been proposed to explain the downstream results of PNPase knockdown in the *C. elegans* model system. To summarize, reduction in PNPase in *C. elegans* is causing a decrease in RNase P which in turn causes an accumulation of mitochondrial polycistronic transcripts. This decreases the available tRNA as well as decreasing the amount of OXPHOS complexes, which interrupts OXPHOS and increases ROS production in the form of superoxides, increasing the lifespan of the animal as well as increasing *fzo-1* expression.

The split in the model is due to the fact that teasing apart these two possibilities, decrease in available tRNA and decrease in OXPHOS complexes, and their effect on interrupted OXPHOS is unlikely. However, it is possible to determine if there is a decrease in the amount of tRNA available via qPCR on extracted mitochondria. The amount of OXPHOS complexes can also be tested via crystallization. It is also possible to test the levels of individual components of the OXPHOS complexes via specific western blots.

While OXPHOS has been measured indirectly via the NAD⁺/NADH ratio, further investigation using a Clark oxygen chamber would give a more accurate picture of respiration in knockdown animals. The increase in ROS has been shown to increase lifespan in knockdown animals, and knockdown animals have an increase in *fzo-1*. To determine if these are

independent results of an increase in ROS, overexpressing *fzo-1* in wildtype animals would show if an increase in *fzo-1* without a corresponding increase in ROS is capable of increasing lifespan.

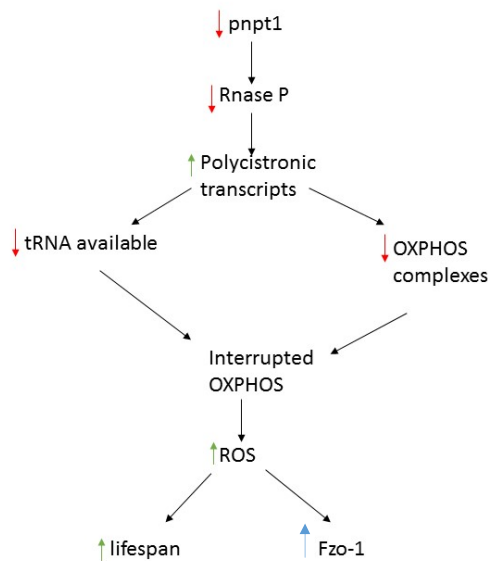


Figure 21: Proposed mechanism for the downstream actions of knockdown of *pnpt-1* in *C. elegans*. It is thought that the decrease in PNPase, and resulting decrease in RNase P, is causing an accumulation of mitochondrial polycistronic transcripts in the mitochondria. This accumulation has two different implications: there is a decrease in the amount of tRNAs available, as they are not being excised from the mitochondrial genome as well as causing a decrease in the OXPHOS complexes. This, in turn, interrupts OXPHOS and increases ROS in the form of superoxides, which, in *C. elegans*, increases lifespan and increases *fzo-1* expression.

Literature Cited

Archer S (2013). Mitochondrial dynamics – mitochondrial fission and fusion in human diseases. *N Engl J Med* 369: 2236-2251.

Balaban RS, Nemoto S, Tinkel T (2005). Mitochondria, oxidants, and aging. *Cell* 120(4): 483-495.

Bordone L and Guarente L (2005). Calorie restriction, SIRT1 and metabolism: understanding longevity. *Nat Rev Mol Cell Biol.* 6(4): 298-305.

Brighton CT and Hunt RM (1974). Mitochondrial calcium and its role in calcification. *Clinical Orthopaedics and Related Research* 100(100): 406-416.

Castandet B, Hotto AM, Fei Z, Stern DB (2013). Strand-specific RNA sequencing uncovers chloroplast ribonuclease functions. *FEBS Letters* 587(18): 3096-3101.

Chen H, Chomyn A, Chan DC (2005). Disruption of fusion results in mitochondrial heterogeneity and dysfunction. *J Biol Chem* 280: 26185-26192

Chen HW, Rainey RN, Balatoni CE, Dawson DW, Troke JJ, Wasiak S, Hong JS, McBride HM, Koehler CM, Teitell MA, French SW (2006). Mammalian polynucleotide phosphorylase is an

intermembrane space RNase that maintains mitochondrial homeostasis. *Mol Cell Biol*, 26(22), 8475–8487.

Das SK, Sokhi UK, Bhutia S, Azab B, Su ZZ, Sarkar D, Fisher PB (2010). Human polynucleotide phosphorylase selectively and preferentially degrades microRNA-221 in human melanoma cells. *Proc Natl Acad Sci U S A*. 107(26): 11948–11953.

de Bono M (2003). Molecular approaches to aggregation behavior and social attachment. *J Neurobiol* 54(1):78-92

Dejean LM, Martinez-Caballero S, Kinnaly KW (2006). Is MAC the knife that cuts cytochrome c from mitochondria during apoptosis? *Cell Death and Differentiation* 13(8): 1387-1395

Dillin A, Hsu AL, Arantes-Oliveira N, Lehrer-Graiwer J, Hsin H, Fraser AG, Kamath RS, Ahringer J, Kenyon C (2002). Rates of behavior and aging specified by mitochondrial function during development. *Science* 298(5602): 2398-2401.

Droge W (2002). Free radicals in the physiological control of cell function. *Physiol Rev*. 82(1): 47-95.

Feng J, Frederic B, Hekimi S (2001). Mitochondrial electron transport is a key determinant of life span in *Caenorhabditis elegans*. *Dev Cell* 1(5): 633-644.

Fesik SW and Shi Y (2001). Controlling the Caspases. *Science*. 294: 1477-1478.

Germain A, Herlich S, Larom S, Kim SH, Schuster G, Stern DB (2011). Mutational analysis of *Arabidopsis* chloroplast polynucleotide phosphorylase reveals roles for both RNase PH core domains in polyadenylation, RNA 3'-end maturation and intron degradation. *The Plant Journal*. 67: 381-394.

Giannakou ME, Goss M, Junger MA, Hafen E, Leevers SJ, Partridge L (2004). Long-lived *Drosophila* with overexpressed dFOXO in adult fat body. *Science* 305(5682): 361

Green DR (1998). Apoptotic pathways: the roads to ruin. *Cell* 94(6): 695-698

Gomes AF, Guimaraes EV, Carvalho L, Correa JR, Mendonca-Lima L, Barbosa HS (2011). Toxoplasma gondii down modulates cadherin expression in skeletal muscle cells inhibiting myogenesis. *BMC Microbiol.* 11: 110.

Ishii N, Fujii M, Hartman PS, Tsuda M, Yasuda K, Senoo-Matsuda N, Yanase S, Ayusawa D, Suzuki K (1998). A mutation in succinate dehydrogenase cytochrome b causes oxidative stress and ageing in nematodes. *Nature* 394(6694): 694-697.

Jang SY, Kang HT, Hwang ES (2012). Nicotinamide-induced mitophagy: event mediated by high NAD⁺/NADH ratio and SIRT1 protein activation. *J Biol Chem* 287(23): 19304-19314.

Kayser EB, Morgan PG, Hoppel CL, Sedensky MM (2001). Mitochondrial Expression and Function of GAS-1 in *Caenorhabditis elegans* *J. Biol. Chem.*, 276: 20551–20558

Kenyon C, Chang J, Gensch E, Rudner A, Tabtiang R (1993). A *C. elegans* mutant that lives twice as long as wild type. *Nature* 366, 461–464

Kenyon C (2005). The plasticity of aging: insights from long-lived mutants. *Cell* 120, 449–460.

Kimura KD, Tissenbaum HA, Liu Y, Ruvkun G (1997). *daf-2*, an insulin receptor-like gene that regulates longevity and diapause in *Caenorhabditis elegans*. *Science* 277(5328): 942-946.

Lee SS, Lee RY, Fraser AG, Kamath RS, Ahringer J, Ruvkun G (2003). A systematic RNAi screen identifies a critical role for mitochondria in *C. elegans* longevity. *Nat Genet* 33: 40-48

Leszczyniecka M, DeSalle R, Kang DC, Fisher PB (2004). The origin of polynucleotide phosphorylase domains. *Mol Phylogenetics Evol* 31(1), 123–130.

Leszczyniecka M, Kang DC, Sarkar D, Su ZZ, Holmes M, Valerie K, Fisher PB (2002). Identification and cloning of human polynucleotide phosphorylase, hPNPase old-35, in the context of terminal differentiation and cellular senescence. *Proc Natl Acad Sci U S A.* 99(26): 16636–16641.

Leszczyniecka M, Su ZZ, Kang DC, Sarkar D, Fisher PB (2003). Expression regulation and genomic organization of human polynucleotide phosphorylase, hPNPase(old-35), a type I interferon inducible early response gene. *Gene*. 316, 143–156

Liu F, Gong J, Huang W, Wang Z, Wang M, Yang J, Wu C, Wu Z, Han B (2014). MicroRNA-106b-5p boosts glioma tumorigenesis by targeting multiple tumor suppressor genes. *Oncogene* 33(40): 4812-4822.

Liu X, Yu J, Jiang L, Wang A, Shi F, Ye H, Zhou X (2009). MicroRNA-222 regulates cell invasion by targeting matrix metalloproteinase 1 (MMP1) and manganese superoxide dismutase 2 (SOD2) in tongue squamous cell carcinoma cell lines. *Cancer Genomics Proteomics* 6(3): 131-139

Lupini L, Bassi C, Ferracin M, Bartonicek N, D'Abundo L, Zagatti B, Callegari E, Musa G, Moshiri F, Gramantieri L, Corrales FJ, Enright AJ, Sabbioni S, Negrini M (2013). miR-221 affects multiple cancer pathways by modulating the level of hundreds of messenger RNAs. *Front Genet* 4:64

Martinou JC and Youle RJ (2011). Mitochondria in apoptosis: Bcl-2 family members and mitochondrial dynamics. *Dev Cell*. 21(1): 92-101.

Miller RJ (1998). Mitochondria – the kraken wakes! *Trends in Neurosci* 21(3) 95-97.

Navarro A and Boveris A (2007). The mitochondrial energy transduction system and the aging process. *Am J Physiol Cell Physiol* 292(2): 670-686.

Pardis S and Ruvkun G (1998). *Caenorhabditis elegans* Akt/PKB transduces insulin receptor-like signals from AGE-1 PI3 kinase to the DAF-16 transcription factor. *Genes Dev* 12(16): 2488-2498.

Piwowarski J, Grzechnik P, Dziembowski A, Dmochowska A, Minczuk M, Stepień P (2003). Human polynucleotide phosphorylase, hPNPase, is localized in mitochondria. *J Mol Biol*, 329(5), 853–857.

Raijmakers R, Egberts W, van Venrooij W, Pruijn GJM (2002). Protein-protein interactions between human exosome components support the assembly of RNase PH-type subunits into a six-membered PNPase-like ring. *J Mol Biol.* 323(4): 653–663

Rainey R, Glavin J, Chen H, French S, Teitell M, Koehler C (2006). A new function in translocation for the mitochondrial i-AAA protease Yme1: Import of polynucleotide phosphorylase into the intermembrane space. *Mol Cell Biol.* 26(22): 8488–8497.

Rambold AS, Kostecky B, Elia N, Lippincott-Schwartz J (2011). Tubular network formation protects mitochondria from autophagosomal degradation during nutrient starvation. *Proc Natl Acad Sci U S A* 108(25): 10190-10195.

Rankin CH (2002). From gene to identified neuron to behavior in *Caenorhabditis elegans*. *Nat Rev Genet.* 3(8): 622-630

Rizzuto R, Marchi S, Bonora M, Aguiari P, Bononi A, De Stefani D, Giorgi C, Leo S, Rimessi A (2009). Ca²⁺ transfer from the ER to mitochondria: when, how, and why. *Biochem Biophys Acta* 1787(11): 1342-1351.

Robb EL, Christoff CA, Maddalena LA, Stuart JA (2013). Mitochondrial reactive oxygen species (ROS) in animal cells: relevance to aging and normal physiology. *Can J Zoo* 92(7): 603-613

Rodriguez M, Snoek LB, De Bono M, Kammenga JE (2013). Worms under stress: *C. elegans* stress response and its relevance to complex human disease and aging. *Trends Genet.* 29(6): 367-374.

Sarkar D and Fisher PB (2006). Human polynucleotide phosphorylase (hPNPase old-35): An RNA degradation enzyme with pleiotrophic biological effects. *Cell Cycle* 5(10): 1080–1084.

Sarkar D and Fisher PB (2006). Molecular mechanisms of aging-associated inflammation. *Can Let.* 236(1): 13–23.

Sarkar D and Fisher PB (2006). Polynucleotide phosphorylase: An evolutionary conserved gene with an expanding repertoire of functions. *Pharm Therap* 112(1): 243–263.

Sarkar D, Lebedeva IV, Emdad L, Kang DC, Baldwin AS, Fisher PB (2004). Human polynucleotide phosphorylase (hPNPase^{old-35}): A potential link between aging and inflammation. *Can Res* 64(20): 7473–7478.

Sarkar D, Park ES, Fisher PB (2006). Defining the mechanism by which IFNbeta downregulates c-myc expression in human melanoma cells: Pivotal role for human polynucleotide phosphorylase (hPNPase^{old-35}). *Cell Death Diff* 13(9): 1541–1553

Sarkar D, Leszczyniecka M, Kang DC, Lebedeva I, Valerie K, Dhar S, Pandita TK, Fisher PB (2003). Downregulation of Myc as a potential target for growth arrest induced by human polynucleotide phosphorylase (*hPNPase^{old-35}*) in human melanoma cells. *J Biol Chem* 278:24542–51

Sarkar D, Park ES, Emdad L, Randolph A, Valerie K, Fisher PB (2005). Defining the domains of human polynucleotide phosphorylase (hPNPase^{old-35}) mediating cellular senescence. *Mol Cell Biol* 25: 7333-7343.

Sarkar D, Park ES, Barber GN, Fisher PB (2007). Activation of double-stranded RNA-dependent protein kinase, a new pathway by which human polynucleotide phosphorylase (*hPNPase^{old-35}*) induces apoptosis. *Cancer Res* 67(17): 7948-7953

Schaffitzel E and Hertweck M (2006). Recent aging research in *Caenorhabditis elegans*. *Exp Gerontol* 41(6): 557-563.

Schulz TJ, Zarse K, Voigt A, Urban N, Birringer M, Ristow M (2007). Glucose restriction extends *Caenorhabditis elegans* life span by inducing mitochondrial respiration and increasing oxidative stress. *Cell Met* 6(4): 280-293.

Sena LA and Chandel NS (2012). Physiological roles of mitochondrial reactive oxygen species. *Mol Cell* 48(2): 158-167.

Shigenaga MK, Hagen TM, Ames BN (1994). Oxidative damage and mitochondrial decay in aging. *Proc. Natl. Acad. Sci. USA* 91: 10771-10778

Shore DE, Carr CE, Ruvkun G (2012). Induction of Cytoprotective Pathways Is Central to the Extension of Lifespan Conferred by Multiple Longevity Pathways. *PLoS Genet* 8(7): e1002792.

Sokhi UK, Das SK, Dasgupta S, Emdad L, Shiang R, DeSalle R, Sarker D, Fisher PB (2013). Human polynucleotide phosphorylase (*hPNPase*^{old-35}): should I eat you or not – that is the question? *Adv Can Res* 119: 161-190.

Sönnichsen B, Koski LB, Walsh A, Marschall P, Neumann B, Brehm M, Alleaume AM, Artelt J, Bettencourt P, Cassin E, Hewitson M, Holz C, Khan M, Lazik S, Martin C, Nitzsche B, Ruer M, Stamford J, Winzi M, Heinkel R, Röder M, Finell J, Häntsch H, Jones SJ, Jones M, Piano F, Gunsalus KC, Oegema K, Gönczy P, Coulson A, Hyman AA, Echeverri CJ (2005). Full-genome RNAi profiling of early embryogenesis in *Caenorhabditis elegans*. *Nature* 434(7032): 462-469.

Stickney L, Hankins J, Miao X, Mackie G (2005). Function of the conserved S1 and KH domains in polynucleotide phosphorylase. *J Bact* 187(21): 7214–7221

Suen DF, Norris KL, Youle RJ (2008). Mitochondrial dynamics and apoptosis. *Genes and Dev* 22:1577-1590

Symmons MF, Jones GH, Luisi BF (2000). A duplicated fold is the structural basis for polynucleotide phosphorylase catalytic activity, processivity, and regulation. *Structure*. 8(11): 1215–1226.

Symmons M, Williams M, Luisi B, Jones G, Carpousis A (2002). Running rings around RNA: A superfamily of phosphate-dependent RNases. *Trend Biochem Sci* 27(1): 11–18

Tacutu R, Shore DE, Budovsky A, de Magalhaes JP, Ruvkun G, Fraifeld VE, Curran SP (2012). Prediction of *C. elegans* longevity genes by human and worm longevity networks. *PLoS One* 7(10): e48282.

Thannickal VJ and Fanburg BL (2000). Reactive oxygen species in cell signaling. *Am J Physiol Lung Cell Mol Physiol.* 279(6): 1005-1028.

Tondera D, Grandemange S, Jourdain A, Karbowski M, Mattenberger Y, Herzig S, Da Cruz S, Clerc P, Raschke I, Merkwirth C, Ehses S, Krause F, Chan DC, Alexander C, Bauer C, Youle R, Langer T, Martinou JC (2009). SLP-2 is required for stress-induced mitochondrial hyperfusion. *EMBO J.* 28(11):1589-600.

Trachootham D, Alexandre J, Huang P (2009). Targeting cancer cells by ROS mediated mechanisms: A radical therapeutic approach? *Nat Rev Drug Discov.* 8:579-591.

Van Maerken T, Sarkar D, Speleman F, Dent P, Weiss W, Fisher PB (2009). Adenovirus-mediated hPNPase(old-35) gene transfer as a therapeutic strategy for neuroblastoma. *J Cell Phys.* 219(3): 707–715

Van Raamsdonk JM and Hekimi S (2010). Reactive oxygen species and aging in *Caenorhabditis elegans*: causal or casual relationship? *Antioxid Redox Signal* 13(12): 1911-1953.

Van Raamsdonk JM and Hekimi S (2012). Superoxide dismutase is dispensable for normal animal lifespan. *Proc natl Acad Sci U S A.* 109(15): 5785-5790.

Vedrenne V, Gowher A, De Lonlay P, Nitschke P, Serre V, Boddaert N, Altuzarra C, Mager-Heckel AM, Chretien F, Entelis N, Munnich A, Tarassov I, Rotig A (2012). Mutation in PNPT1, which encodes a polyribonucleotide nucleotidyltransferase, impairs RNA import into mitochondria and causes respiratory-chain deficiency. *Am J hum Genet* 91(5): 912-918.

Von Ameln S, Wang G, Boulouiz R, Rutherford MA, Smith GM, Li Y, Pogoda HM, Nurnberg G, Stiller B, Volk AE, Borck G, Hong JS, Goodyear RJ, Abidi O, Nurnberg P, Hofmann K, Richardson GP, Hammerschmidt M, Moser T, Wollnik B, Koehler CM, Teitell MA, Barakat A, Kubish C (2012). A mutation in PNPT1, encoding mitochondrial-RNA-import PNPase, causes hereditary hearing loss. *Am J Hum Genet* 91(5): 919-927.

Walker G, Houthoofd K, Vanfleteren JR, Gems D (2005). Dietary restriction in *C. elegans*: from rate-of-living effects to nutrient sensing pathways. *Mech. Ageing Dev.* 126: 929–937

Wang G, Chen H, Oktay Y, Zhang J, Allen E, Smith G, Fan KC, Hong JS, French SW, McCaffery JM, Lightowlers RN, Morse HC, Koehler CM, Teitell MA (2010). PNPASE regulates RNA import into mitochondria. *Cell* 142(3): 456–467.

Wang G, Shimada E, Koehler C, Teitell M (2012). PNPASE and RNA trafficking into mitochondria. *Bioch Biophys Acta* 1819(9–10): 998–1007.

Weinberg F and Chandel NS (2009). Mitochondrial metabolism and cancer. *Annals of NY Acad Sci.* 1177: 66-73.

Wong A, Boutis P, Hekimi S (1995). Mutations in the *clk-1* gene of *Caenorhabditis elegans* affect development and behavioral timing. *Genetics* 139: 1247–1259

Yang W and Hekimi S (2010). Two modes of mitochondrial dysfunction lead independently to lifespan extension in *Caenorhabditis elegans*. *Aging Cell* 9: 433-447.

Yang W and Hekimi S (2010). A Mitochondrial superoxide signal triggers increased longevity in *Caenorhabditis elegans*. *PLoS Biol* 8(12): e1000556.

Youle RJ and van der Bliek AM (2012). Mitochondrial fission, fusion, and stress. *Science* 337:1062-1065

Zarse K, Schmeisser S, Groth M, Priebe S, Beuster G, Kuhlow D, Guthke R, Platzer M, Kahn CR, Ristow M (2012). Impaired insulin/IGF1 signaling extends life span by promoting mitochondrial L-proline catabolism to induce a transient ROS signal. *Cell Metab.* 15: 451–465

VITA

Laura Lambert was born 20 June 1986 in Arlington, Texas. She graduated from the University of Virginia in 2008, receiving a Bachelor of Science in Biology and a Bachelor of Arts in Spanish. She received her Masters of Arts in Teaching from James Madison University in 2010.

APPENDIX: Supplementary Protocols

Transformation: Thaw competent cells on ice while chilling a 1.5 mL tube. Aliquot 50 uL cells into chilled tubes; add 5 uL ligation mix to cells. Incubate on ice, 30 minutes. Heat-shock at 42°C for 60 seconds. Incubate on ice, 2 minutes. Add 0.95 mL room temperature LB and shake at 225 rpm for 1 hour at 37 °C. Plate on selective plates.

Pouring NGM plates: In a 1L flask, mix 3 g NaCl, 17 g BactoAgar, and 2.5 g BactoPeptone. Add 975 ml H₂O. Autoclave. Allow to cool for ~30 minutes. Add 1 ml 1 M CaCl₂, 1 ml 5 mg/ml cholesterol in ethanol, 1 ml 1 M MgSO₄ and 25 ml 1 M KPO₄. Swirl to mix. Using a pump or pipette, dispense NGM solution into sterile plates; 10 mL in a 6 cm plate.

Pouring NGM+Carbenicillin plates: As above. Add 100mg carbenicillin prior to pouring.